Spring 2014

Characterization of atrazine transport across nasal respiratory and olfactory mucosae

Wisam Saad Hasan Al Bakri
University of Iowa

CHARACTERIZATION OF ATRAZINE TRANSPORT ACROSS NASAL RESPIRATORY AND OLFACTORY MUCOSA

by

Wisam Saad Hasan Al Bakri

A thesis submitted in partial fulfillment
of the requirements for the Master of
Science degree in Pharmacy
in the Graduate College of
The University of Iowa

May 2014

Thesis Supervisor: Professor Maureen D. Donovan

Graduate College
The University of Iowa
Iowa City, Iowa

CERTIFICATE OF APPROVAL

_____

MASTER'S THESIS

_____

This is to certify that the Master's thesis of

Wisam Saad Hasan Al Bakri

has been approved by the Examining Committee
for the thesis requirement for the Master of Science
degree in Pharmacy at the May 2014 graduation.

Thesis Committee: _____
Maureen D. Donovan, Thesis Supervisor

_____
Douglas R. Flanagan

_____
Jennifer Fiegel

To my parents for unconditionally providing their love and support.

ACKNOWLEDGMENTS

I would like to express my sincere thankfulness and gratitude to my advisor Professor Dr. Maureen Donovan. Thank you for your guidance. You have absolutely been a pleasure to work with. Your patience, smile, and sense of humor are truly remarkable. Thank you for sharing them so generously with me along the way.

I would like to thank Professor Dr. Douglas R. Flanagan for his stimulating discussions and suggestions. Thanks Dr. for being always welling to help me whenever I asked.

I would also like to express my gratitude and respect to my committee member Professor Dr. Jennifer Fiegel for serving my committee member, for her time and effort in reviewing this work.

I am deeply and forever indebted to my senior graduate student Ana Catalina Ferreira for her endless help. Ana, you have patiently listened to me complain about my work. Thank you for being such a wonderful friend, who accepts, cares and understands me.

I would like to acknowledge the financial and technical support of the Higher Committee of education development in Iraq (HCED) and it is staff.

I would like to thank my labmates, Namita, Shanthi, Bhanu and Jiaqiang, for making this research time fun for me.

Also, I would like to thank Kawther, Ali and Diar for being my small family from the first day I arrived to Iowa City.

Finally I would like to thank my family for their endless love and support. Thanks for supporting me during my study and believing on me. Mom and Dad, you are wonderful parents and wonderful friends.

ABSTRACT

Atrazine (ATZ) is one of the most commonly used herbicides in the United States. Atrazine was banned by the European Union in 2005 because of its ubiquity in drinking water, but, in The United States more than 75 million pounds of atrazine are used annually, especially in the Midwest. Atrazine has many adverse health effects including enhancing developmental, immunologic and endocrine alterations. Studies have reported that exposure to atrazine causes dopaminergic toxicity and mitochondrial dysfunction; these cellular changes have been linked to an increase in the incidence of Parkinson's disease.

The objective of this study was to characterize atrazine's effect on the respiratory and olfactory mucosae with specific attention to the potential for atrazine transfer to the brain via the olfactory system. Uptake of atrazine was investigated across excised nasal mucosal tissues equilibrated in Krebs's Ringer's buffer (KRB) or in a co-solvent system containing propylene glycol (PG), similar to the commercial herbicide product. Active uptake pathways were probed using 2,4-dinitrophenol (2,4-DNP) as a metabolic inhibitor. Brightfield microscopy was used to assess the effects of atrazine exposure on the tissues.

Atrazine was found to be transported across the nasal tissues in a manner consistent with passive diffusion; 2,4-DNP did not reduce the overall uptake of ATZ. Microscopy showed erosion of the epithelial surface following exposure to ATZ-PG-KRB compared to control and ATZ -KRB. These results suggest a negative effect of the ATZ co-solvent formulations on nasal tissues which may contribute to increase systemic and CNS exposure.

TABLE OF CONTENTS

LIST OF FIGURES

CHAPTER 1

INTRODUCTION

The use of herbicides has grown during the last 30 years. Environmental exposure for humans to agrichemicals is common and results in both acute and chronic health effects. These include acute and chronic neurotoxicity, lung damage, chemical burns and cancer[1]. Pesticides can be inhaled directly in large amounts when they are being sprayed or handled either by the applicators or by residents in the exposure area. For inhalation exposure to herbicides, nearly all droplets which are larger than 10 μm in size are deposited in the nasal cavity; this subsequently results in a rapid and high systemic absorption of pesticide due to the relatively large absorptive surface of the nasal epithelium, the thin and highly vascular nature of the blood vessels and the high local blood flow[2].

Triazine herbicides, such as atrazine, are the most heavily used agricultural chemicals in the United States due to their application flexibility and the ability to mix them with other herbicides[3]. These herbicides are used for both post-emergence and pre-emergence control of annual grassy and broadleaf weeds in corn and other crops[4]. Atrazine was banned in the European Union in 2005 because of its ubiquity in drinking water [5]; however, in the United States, more than 75 million pounds of atrazine are applied annually to corn and sorghum crops primarily in the Midwest [6]. This heavy use occurs despite the fact that atrazine is the most commonly reported ground and surface water contaminant in the US[7].

Atrazine, 6-chloro-4-N-ethyl-2-N-propan-2-yl-1,3,5-triazine-2,4-diamine (Figure 1-1) is an odorless, white crystalline solid[8]. Atrazine has a logP value of 2.6 and pK_a of 1.6[8]. Atrazine acts by inhibiting the primary events in photosynthesis in the chloroplast by binding to the D-1 protein in the photosynthetic electron transport chain. This binding stops the transfer of electrons from photosystem I to photosystem II which is essential for the production of photosynthetic energy[9].

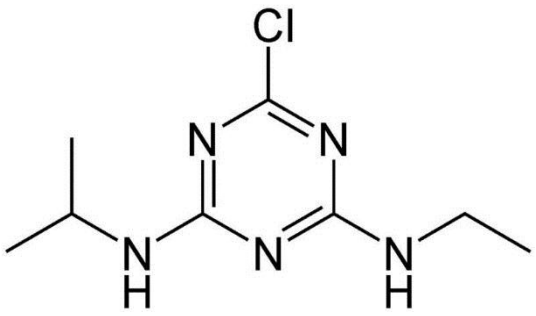

Figure 1-1 Chemical structure of atrazine.

The metabolism of atrazine is complex and results in many metabolites (Figure1-2). Many human and animal studies have investigated the metabolism of atrazine and the results demonstrate a variety of metabolites and metabolic pathways[10]. Atrazine is primarily metabolized by cytochrome P450 and to a lesser extent by phase II glutathione transferases [11,12,10]. CYP1A2 and CYP2C19 are the major liver enzymes involved in phase I reactions forming desethyl atrazine (DEA) and desisopropyl atrazine (DIA). CYP3A4, at high concentrations of atrazine, also produces both DEA and DIA[13]. Didealkyl atrazine (DACT), the most frequently detected urinary metabolite of atrazine is used as an indicator to assess an individual's exposure to atrazine, and is produced by dealkylation of DIA and DEA by CYP1A1 [14,15]. Both cytochrome P-450 and glutathione transferase are expressed in the nasal epithelium and thus may play a role in the conversion of atrazine to active and inactive metabolites following inhalation[16].

Atrazine has been associated with many adverse health effects in humans and animals. Preliminary studies in humans have shown that exposure to atrazine, even at levels below the Maximum Contaminant Levels (MCL) approved by US Environmental Protection Agency (EPA) is associated with menstrual irregularities[17]. Atrazine is a potent endocrine disruptor and there are increasing numbers of studies reporting that animal exposure to atrazine is associated with reproductive, developmental and immunological alterations[6,16,17,18,19].

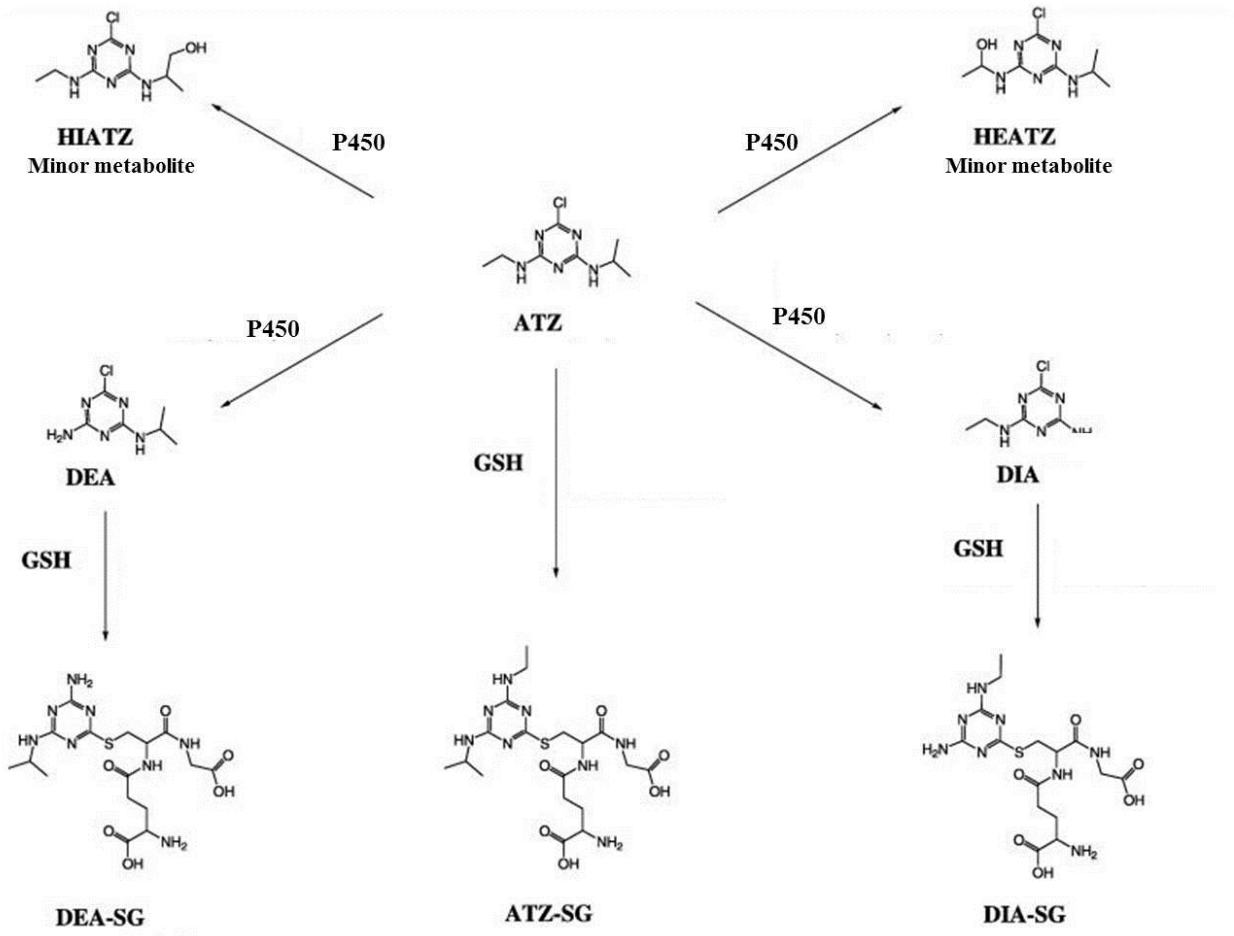

Figure 1-2 Metabolism of atrazine in mammals (adapted with permission[13]). Atrazine is metabolized primarily by cytochrome P450 and to a much lesser extent by glutathione transferase (GSH). *Abbreviations:* Atrazine (ATZ), desisopropyl atrazine (DIA), desethyl atrazine (DEA), atrazine-glutathione (ATR-SG), 2-hydroxyethylatrazine (HEATZ), 1-hydroxyisopropylatrazine (HIATZ). desisopropyl atrazine-glutathione (DIA-SG) and desethyl atrazine-glutathione (DEA-SG).

Recently, a number of studies have shown an association between the inhalation exposure of atrazine and the risk of Parkinson's disease[22]. A study reported by Curwin *et al.* reported that not only atrazine applicators, but also their families, are at risk of developing Parkinson's disease. The proposed mechanism of action of atrazine and some of its metabolites on dopaminergic neurons is shown in Figure 1-3. Atrazine has been reported to be a potential basal ganglia toxicant and its oral and inhalation exposure is associated with dopaminergic neurotoxicity manifested by decreased striatal dopamine levels[21,22,23]; the mechanism behind this reduction is largely unknown. A study conducted by Filipov *et al.* reported that atrazine and two of its major metabolites, DIA and DEA, decrease striatal dopamine levels and alter dopamine homeostasis. Atrazine and DEA promote dopamine uptake into the synaptosomes by the activation of the dopamine transporter (DAT), which is responsible for the transport of dopamine from the synaptic cleft into the presynaptic nerve terminals. Additionally, atrazine, DEA and DIA inhibit vesicular monoamine transporter (VMAT-2), which is responsible for the transport of dopamine from the cytosol into the synaptic vesicles for storage and protection from oxidation. These two mechanisms result in excessive accumulation of cytosolic dopamine which in turn generates oxidative stress by producing reactive oxygen species such as dopamine quinone[24]. In addition, excessive accumulation of dopamine in the cytosol also inhibits mitochondrial respiration which, in turn, can cause neuro-degeneration associated with Parkinson's disease[26]. The overall effect of atrazine exposure results in a dose-dependent increase in the DAT/VMAT-2 uptake ratio; such an increase is used as an indication of individual neuronal susceptibility to toxicants[27].

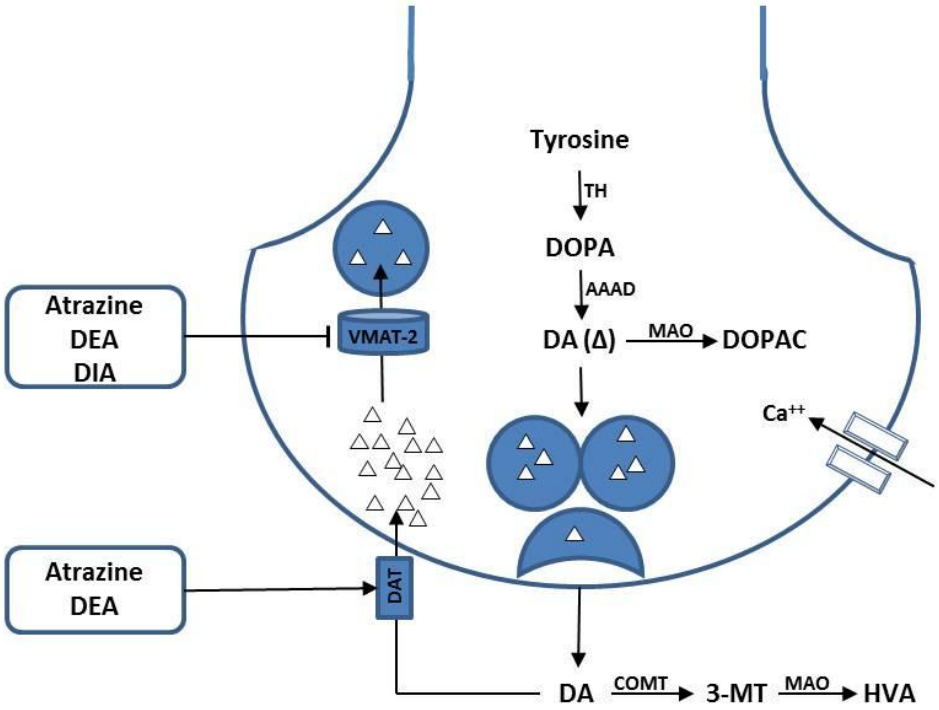

Figure 1-3 Proposed mechanism of action of atrazine on dopaminergic neurons (reproduced with permission[24]). Atrazine, DEA and DIA alter DA homeostasis by inhibiting VMAT-2 resulting in increased cytosolic DA. Additionally, atrazine and DEA increase synaptosomal dopamine reuptake by activating DAT. *Abbreviations*: Desethyl atrazine (DEA), desisopropyl atrazine (DIA), dopamine (DA), tyrosine hydroxylase (TH), aromatic amino acid decarboxylase (AAAD), monoamine oxidase (MAO), catechol-O-methyltransferase (COMT), dopamine transporter (DAT), vesicular monoamine transporter-2 (VMAT-2), 3,4-dihydroxyphenylacetic acid (DOPAC), homovanillic acid (HVA) and 3-methoxytyramine (3-MT).

Anatomy and Physiology of the Nose

The nasal cavity is divided into two halves by the septum, which serves as a central structural support of the nose[28]. Each half of the nose consists of the floor, septum and lateral wall. There are three nasal turbinates protruding from each lateral side of the nasal cavity; they are referred to as the superior, middle and inferior turbinates (Figure 1-4). Turbinates protrude into the nasal cavity and are covered with a secretory epithelium covered with mucus; they provide an increased surface area of the lining of the nose and assist in humidification, filtration and cleaning of air flowing through the nose[29]. The nose has two primary functions: the first is olfaction – the sense of smell, and the second function is conditioning of the inspired air by filtration, heating and humidification[30].

Each chamber of the nasal cavity can be divided into three regions[31]:

(1) Nasal vestibule, which is the dilated entryway into the nasal cavity and is lined by stratified squamous epithelium.

(2) Respiratory region, which is the largest region of the nasal cavities and is lined by the respiratory mucosa.

(3) Olfactory region, which is located at the apex of each nasal cavity and is lined by the specialized olfactory mucosa.

The nasal vestibule is lined with squamous epithelium with sebaceous and sweat glands[32]. This, and a transitional epithelium, is also found at the anterior tips of the middle and inferior turbinates. In the posterior two thirds of the nasal cavity, a pseudostratified columnar epithelium (respiratory epithelium) is found, which is composed of four major cell types: ciliated (columnar) cells, non-ciliated (columnar) cells, goblet cells, and basal cells.

The superior turbinate and adjacent septum is covered with a pseudostratified epithelium containing olfactory cells (bipolar neurons acting like peripheral receptors and first-order ganglia), basal cells, and Bowman's glands (small serous tubulo-alveolar glands)[33].

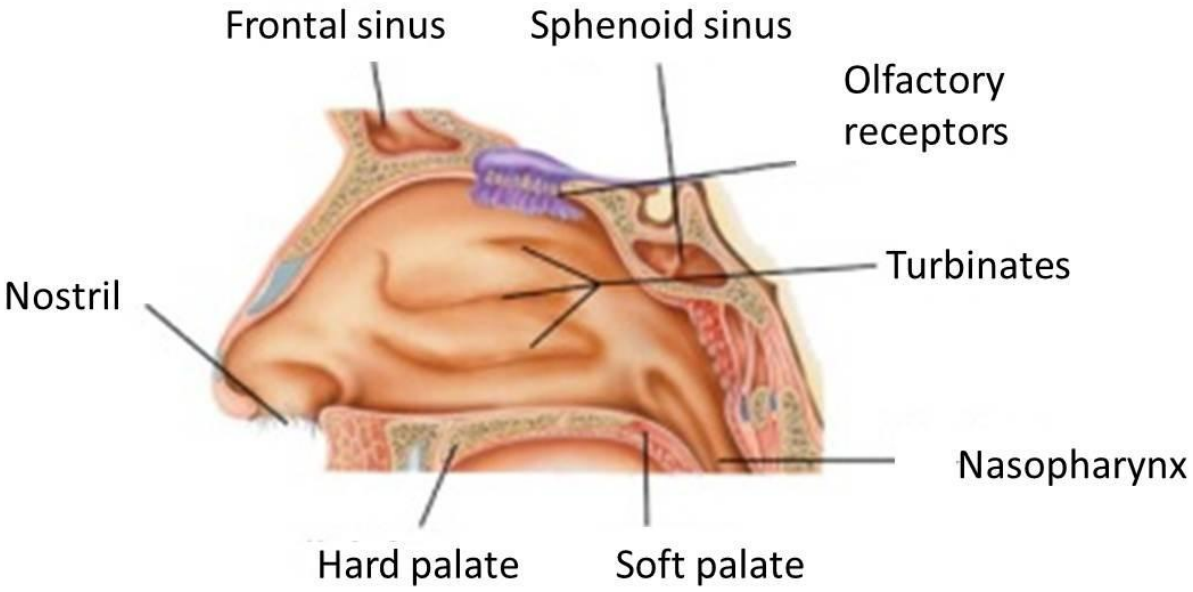

Figure 1-4 Schematic representation of a sagittal section of the nasal cavity[34].

Nose to Brain Transport

There are several transport pathways by which the drugs administered nasally can reach the central nervous system (CNS), brain and cerebrospinal fluid (CSF). These are shown schematically in Figure 1-5. Normally when drugs are administerd nasally, they will be rapidly absorbed into the bloodstream, cleared by mucocilliary clearance or metabolized by the enzymatic population in the nasal mucosa[16,35]. For drugs absorbed systemetically, the drug is cleared by normal clearance mechanisms; however, once the drug is in the systemic circulation, it can reach the CNS by crossing the blood-brain barrier (BBB) either by trancellular transport if it is sufficiently lipophilic or by specific transport mechanisms[36,37]. Drugs may also be transported directly to the brain from the nasal olfactory region via the olfactory pathway. There are also many different pathways by which the drug molecules can traverse the olfactory epithelium to the CNS[38]. The paracellular transport pathway involves transport through the tight junctions between the sustentacular cells, or the cleft between the sustentacular cells and the olfactory neurons. Axonal transport, where the drug is taken up into the primary neurons of the olfactory epithelium by endocytosis or pinocytosis, may also play a role in the nose to brain transport. The trigeminal nerve pathway has also been identified by Thorne *et al*. as an important pathway for rhe delivery of drugs from the nasal cavity to the CNS[39]. The trigeminal nerve innervates the respiratory and olfactory epithelium and terminates in the CNS in the pons. Recently there has been convincing evidence that intranasal administration of radiolabeled proteins such as insulin-like growth factor (^{125}I-IGF-I) results in high concentration of radioactvity in the trigeminal nerve branches, ganglion, pons and olfactory bulbs[39]. Transcellular transport across sustentacular cells, either by passive diffusion, active transport or receptor-mediated endocytosis is also a potential transport pathway from the nose to the brain. Several transporters have been identified in the bovine respiratory and olfactory epitheluim which have been shown to play a role in the uptake of drugs across the nasal mucosa and thus, enhancement of nose to brain transport. The investigation of the role of uptake transporters in bovine mucosal tissues has identified that the large amino acid transporter (LAT-1), dopamine transporter (DAT)

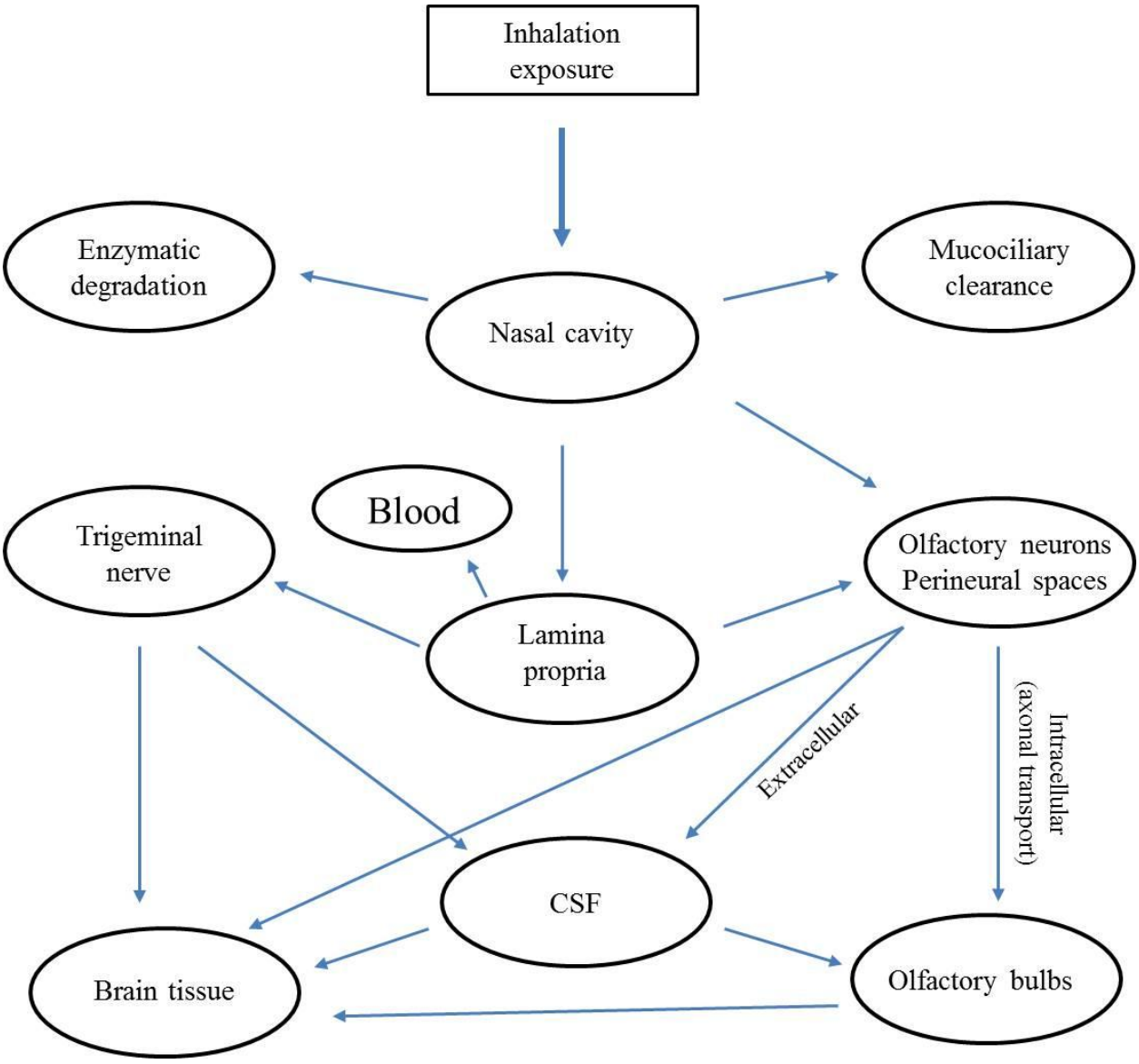

Figure 1-5 Proposed nose-to-brain transport pathways (adapted with permission[40]). Inhaled drugs that reach the nasal cavity are primarily cleared by mucociliary clearance or the enzymatic degradation of the nose. Part of the inhaled drug can be absorbed into the systemic circulation by the respiratory epithelium and potentially cross the blood-brain barrier if it is lipophilic. Drugs may also be transported to the brain if they are deposited into the olfactory region or by the trigeminal nerve pathway.

and organic cation tranporters (OCT1/2) are expressed in bovine olfactory tissues and each plays a role in increasing the uptake of the substrates from the olfactory epithelium into the the olfactory bulb and subsequently to the brain[41,42,43]. The goal of this study is to investigate the uptake of the herbicide, atrazine, which has been associated with Parkinson's disease, across the nasal epithelium. Studying transport through the nasal tissues to determine whether direct transport to the brain through the olfactory epithelium occurs, may provide important new information about the potential for the enhanced toxicity of inhaled atrazine.

CHAPTER 2

OBJECTIVES

For atrazine, an aerosolized herbicide, there is a high risk of inhalation exposure through the nasal cavity. Since atrazine is moderately lipophilic, much of the inhaled dose will likely be transported across the respiratory and olfactory mucosa to the systemic circulation or to the brain. The primary objective of this study was to characterize the biomolecular processes controlling atrazine transport across nasal tissues. This was investigated through the following specific aims:

1. Perform *in vitro* transport studies to probe the transfer rate and concentration dependence of atrazine flux across the bovine olfactory and respiratory mucosae.

2. Evaluate the effect of non-specific metabolic inhibitors on any energy-dependent transport processes for atrazine across bovine nasal mucosal explants.

3. Investigation of the effect of the co-solvents which are added to commercial atrazine formulations on the rate of atrazine transfer across bovine nasal mucosae and artificial membranes.

4. Assessment of the integrity of the bovine mucosal explants exposed to atrazine by histological analysis and using *in vitro* measurement of Lucifer Yellow (LY) permeability as a paracellular transport marker.

CHAPTER 3

MATERIALS AND METHODS

Chemicals

Atrazine, 2,4-dinitrophenol (2,4-DNP), ammonium acetate, Lucifer Yellow dilithium salt and propylene glycol were obtained from the Sigma Chemical Co. (St. Louis, MO). Chemicals and stains used in microscopy were obtained from the Central Microscopy Research Facility, The University of Iowa. Kreb's Ringer's buffer (KRB) salts and acetonitrile for HPLC analysis were obtained from Fisher Scientific. Kreb's Ringer's buffer (KRB) solution containing 1.67 mM $MgCl_2.6H_2O$, 4.56 mM KCl, 119.78 mM NaCl, 1.5 mM $NaH_2PO_4.H_2O$, 0.83 mM Na_2HPO_4 and 10 mM D-glucose, 15 mM $NaHCO_3$ and 1.2 mM $CaCl_2.2H_2O$ was prepared by dissolving these salts in 900 mL of deionized water with the exception of $CaCl_2.2H_2O$. Carbogen gas composed of 95% O_2 + 5% CO_2 was bubbled through the solution for 15~20 min. to lower the solution pH slightly followed by the addition of the $CaCl_2 \cdot 2H_2O$. The volume of the solution was completed to 2 liter with deionized water and the pH was adjusted to 7.4 using HCl or NaOH (1 N). Atrazine solutions over the concentration range of 46.3µM-139.1µM and, 2,4-DNP (1 mM) solutions were prepared by dissolving these compounds in KRB at room temperature.

Experimental Procedures

HPLC Analysis

The samples withdrawn from the diffusion apparatus were analyzed immediately. HPLC analysis was carried out using an Agilent1100 system (Agilent Technologies Co., Santa Clara, CA) consisting of a G1311A quaternary pump, G1313 ALS autosampler and G1315B diode array detector. A Zorbax® C18 column (4.6mm x 250mm) (Agilent Technologies Inc., Lexington, MA) protected by a Phenomenex Gemini–NX C18 (4 x 2.0 mm ID) guard cartridge

system (Agilent Technologies Inc., Lexington, MA) were used to quantify atrazine. The mobile phase was acetonitrile:1 mM ammonium acetate (75:25, v/v) used at a flow rate of 1.4 mL/min. UV detection was at 226 nm. The retention time of atrazine was 4.6 min and the detection was linear in the range from 0.525 µM to 139.1 µM. A calibration curve for atrazine in KRB is shown in Figure 3-1 and a sample chromatogram is presented in Figure 3-2.

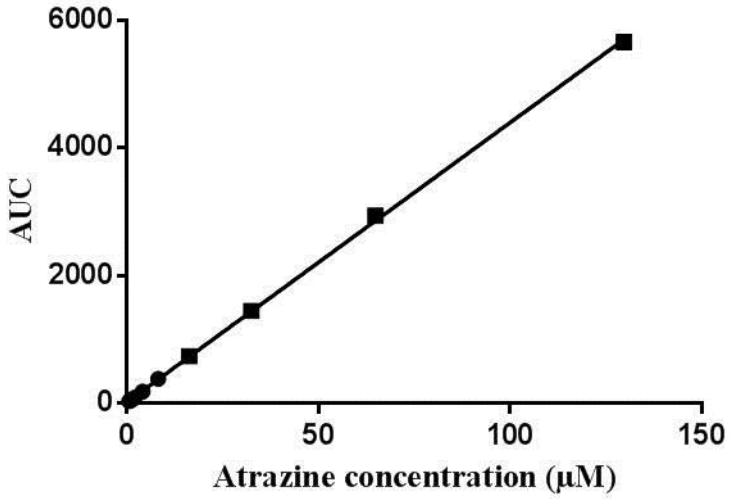

Figure 3-1 Calibration curve for atrazine in KRB. Injection volume = 35µl, linear regression of the data for the calibration curve gave y = 132.02x + 12.8, r^2= 0.99.

.

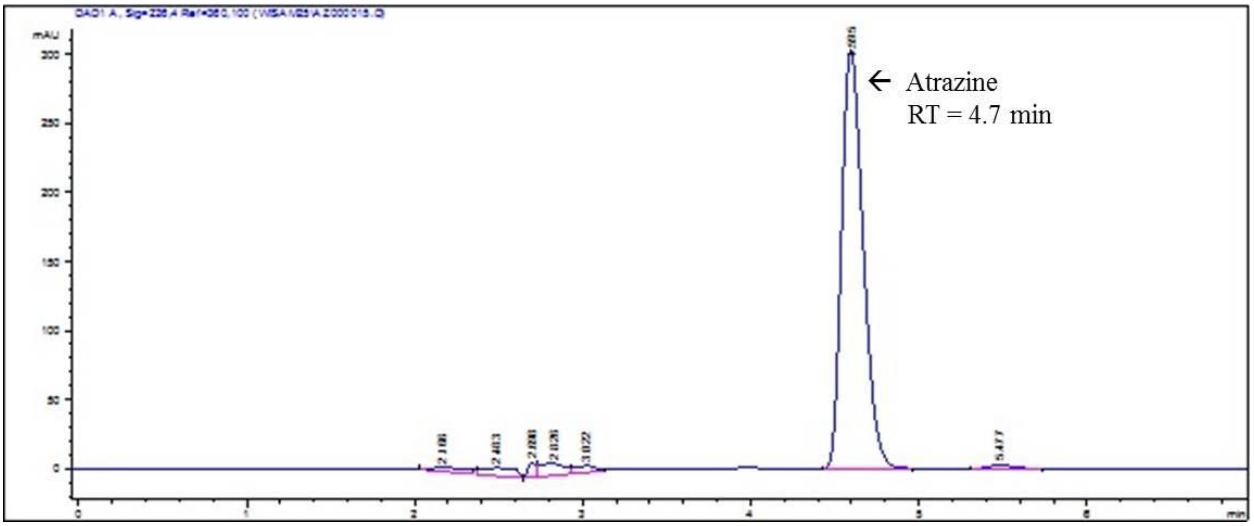

Figure3-2 HPLC chromatogram of atrazine (92.7 µM) in KRB. Mobile phase acetonitrile:1 mM ammonium acetate (75:25, v/v); Column Zorbax® C18 (4.6 mm x 250 mm, 5 µm); flow rate: 1.4 mL/min; wavelength: 226 nm.

Solubility Studies

Excess atrazine was added to three vials, one containing 10 mL KRB buffer, a second containing 5 mL KRB buffer + 5 mL propylene glycol and a third containing 9.5 mL KRB buffer + 0.5 mL propylene glycol. The vials were mixed continuously at 100 rpm using a VWR® incubating orbital shaker (Henry Troemner LLC, Thorofare, NJ) for 72 hours at 25°C. The contents were centrifuged using an Eppendorf® AG5810R centrifuge (Hamburg, Germany) at 26.5 g for 15 minutes, and the resulting supernatant solution was collected and filtered using Millex®-GS (0.22µm) filter units. The filtrate was analyzed by HPLC. A representative calibration curve of atrazine dissolved in 95% KRB buffer + 5% propylene glycol mixture is shown in Figure 3-3.

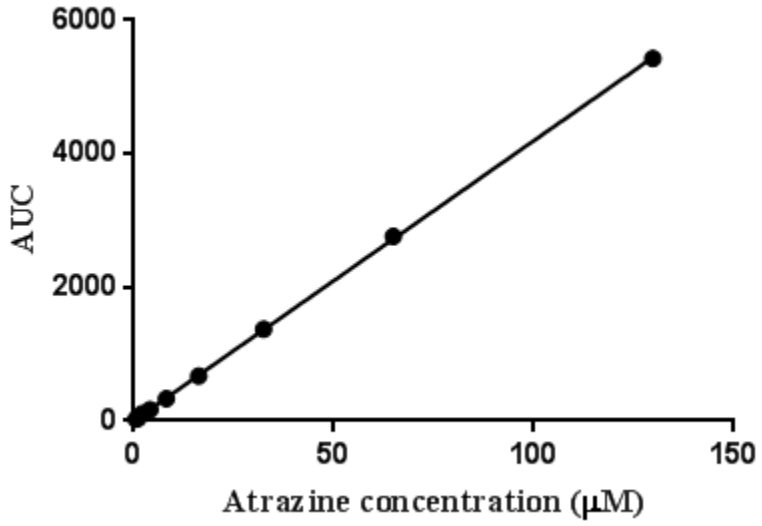

Figure 3-3 A representative calibration curve for atrazine dissolved in 95% KRB + 5% propylene glycol, linear regression of the data gave $y = 41.91x + 5.01$, $r^2 = 0.99$.

Preparation of Mucosal Tissues

Bovine olfactory and respiratory mucosae were obtained from Bud's Custom Meats Co. (Riverside, IA). A longitudinal incision was made along the septal wall of the nasal cavity and a vertical incision was made along the ocular plane to harvest both olfactory and respiratory mucosae. The excised tissues were placed in a fresh ice-Kreb's buffer solution and transported to the lab. The tissue was used within 1 hour of it being excised.

In Vitro Transport Studies

The excised respiratory and olfactory tissues were processed to be ready for the transport experiment by gently rinsing the tissues with KRB solution, cutting them into segments of $1cm^2$ and removing the underlying cartilage. The transport of atrazine across the respiratory and olfactory tissues was studied using Navicyte® (1 mL) vertical diffusion cells (Harvard Apparatus, Holliston, MA). The excised tissues were mounted between the chambers with a diffusional cross sectional area of 0.64 cm^2 to measure the flux across the respiratory and olfactory mucosae. The tissue explants were allowed to equilibrate for 20 min at 37°C by circulating water through a heating manifold (Harvard Apparatus, Holliston, MA) using a Lauda® RM6 water bath (Brinkman Instrument Co., New York, NY). The tissues were exposed to carbogen to provide oxygen and CO_2. After equilibrium, the donor solution was replaced with atrazine dissolved in KRB (1 mL) and the receiver solution was replaced with KRB (1 mL). The experiment was repeated for various atrazine concentrations ranging from 46.3 µM to 139 µM.

Flux Measurement

The amount of atrazine accumulated in the receiver chamber at each time point was measured by HPLC using the appropriate calibration curve (Figure 3-1). The amount of atrazine removed from the receiver chamber from each sample was measured by calculating the amount of atrazine in a 200 µL sample withdrawn at each time point. The cumulative amount of atrazine transferred across the membrane at each time was calculated by adding the cumulative amount of atrazine in the receiver samples to the measured amount of atrazine in the receiver chamber at

each time point. Fick's second law solved under the following conditions (Equation 3-1): (i) initial conditions of C_d = added donor concentration; C_r = 0 at steady state with sink conditions, C_r = 0 was used to calculate the permeability of atrazine across nasal membrane. Analyte flux (J) was calculated (Equation 3-2) by dividing the slope of the steady-state portion of the cumulative amount of atrazine transported vs. time curve (Figure 3-4) by the cross-sectional area exposed to the donor chamber (0.64 cm^2). The permeability of atrazine was determined by dividing the measured flux by the donor concentration (Equation 3-3). The Cumulative amounts of atrazine in the receiver chamber versus time plots are presented in Appendix C.

$$J = \frac{\Delta M_R}{A\Delta t} = P_e \text{ x } (C_d - C_r) \qquad \text{Equation 3-1}$$

Where, $P_e = \frac{D \times K}{h}$

Since, $C_r = 0$ then $J = \frac{\Delta M_R}{A\Delta t} = P_e \times C_d$ Equation 3-2

$$P_e = \frac{J}{C_d} \qquad \text{Equation 3-3}$$

$\Delta M_R/\Delta t$ = Slope of the steady-state portion of the cumulative amount of atrazine vs. time curve.

J = Flux (mass transported across barrier per unit time) (µg/cm^2/min)

K = partition coefficient

D = diffusion coefficient (cm^2/min)

h = membrane thickness (cm)

A = surface area of the tissue available for diffusion (0.64 cm^2)

P_e = permeability coefficient of the solute (cm/min)

M_R = Cumulative amount of solute transported across the tissue (measured amount + removed amount).

C_d = solute concentration in the donor chamber (µg/mL)

C_r = solute concentration in the receiver chamber (µg/mL)

C_d-C_r represents the concentration gradient across the tissue and is approximated by C_d under sink conditions.

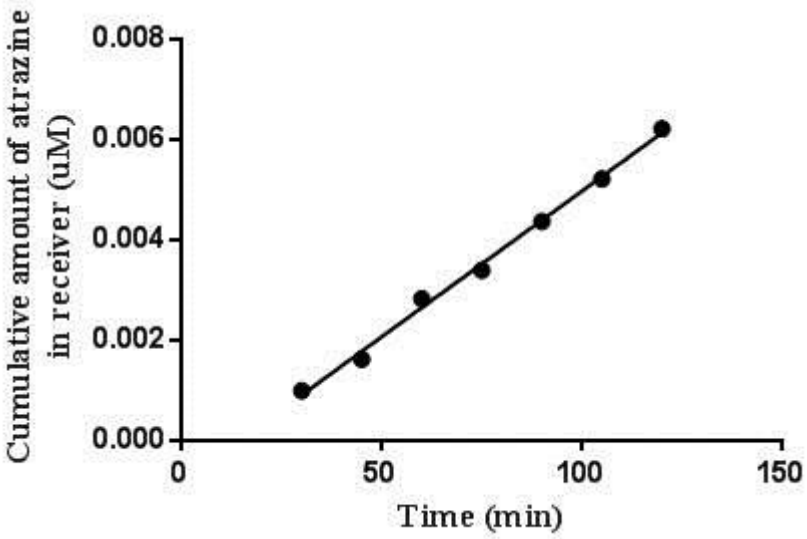

Figure 3-4 A representative plot of the cumulative amount of atrazine (69.5µM) transported across a bovine respiratory tissue explant as a function of time. Linear regression of the data gave: y = 0.058x - 0.84, r2= 0.99.

Transport Inhibitor Studies

The effect of 2,4-DNP on atrazine transport was studied by equilibrating the tissues with 1 mM 2,4- DNP dissolved in KRB for 30 min in both the donor and the receiver chambers. After equilibration, the donor was replaced with 92.7 µM atrazine + 1mM 2,4- DNP dissolved in KRB, and the receiver was replaced with 1mM 2,4- DNP in KRB. TEER values of 2,4- DNP-exposed tissues are presented in Appendix B.

Co-solvent Studies

In order to estimate the effect of the co-solvent contained in the commercial atrazine products on the flux of atrazine across nasal tissues, propylene glycol, which is used as a co-solvent in one of the commercial atrazine products (Brozine®) was studied. Two atrazine solutions were prepared, one containing 92.7 µM atrazine dissolved in KRB + propylene glycol (50:50) and the other composed of 92.7 µM atrazine dissolved in KRB + propylene glycol (95:05). Transport studies were performed by replacing the receiver solution with the KRB + propylene glycol mixture and the donor with atrazine dissolved in a mixture with the same ratio of KRB + propylene glycol. TEER values for tissues used during the transport studies are presented in Appendix B.

Tissue Viability Studies

Transport studies were completed within approximately 4 hours of excision of the nasal tissues. It has been shown that the excised nasal tissues can remain viable for about 4 hours [44]. The integrity of the mucosal tissues was checked by measuring the transepithelial electrical resistance (TEER) using an EVOM^2 epithelial volt-ohmmeter (World Precision Instruments Inc., Sarasota, FL). The measurements were performed before adding atrazine solution to the donor side, immediately after adding it and at the end of the transport experiment. Resistance values less than 100 Ω cm^2 were taken to be an indication of tissue damage and tissue explants showing such low values were discarded. TEER values for tissues exposed to atrazine dissolved in KRB;

2,4- DNP; 50% KRB + 50% propylene glycol; and 95% KRB + 5% propylene glycol are presented in Appendix B.

Lucifer Yellow (LY), a paracellular transport marker, was also used to assess the integrity of the respiratory and olfactory tissues. At the end of one transport study, the tissues were allowed to equilibrate with pre-warmed water for 30 min. Then LY (100 µM) solution (1 mL) was replaced into the donor chamber and fresh water (1 mL) was added to the receiver chamber for a study where respiratory or olfactory tissues were exposed to KRB (control); atrazine (92.7 µM) in KRB; atrazine (92.7 µM) in KRB+ propylene glycol (50:50); and atrazine (92.7 µM) in KRB+ propylene glycol (95:05). The LY experiment was run for an additional hour with continuous aeration with 95% O_2 + 5% CO_2 at a rate of 3-5 bubbles per second at 37°C. The concentration of LY in the receiver chamber at the end of experiment was measured by fluorescence spectroscopy (PerkinElmer Inc., Waltham, MA) using an excitation wavelength of 437.5 nm and an emission wavelength of 527 nm. Transport of more than 1% LY into the receiver chamber, relative to the LY concentration in the donor chamber, indicates that the tissues were compromised[45]. A representative calibration curve of LY solution is shown in Figure 3-5.

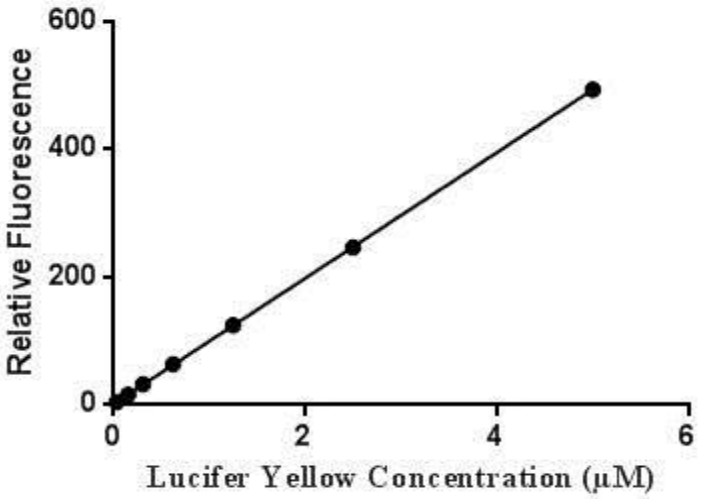

Figure 3-5 Calibration curve for Lucifer Yellow determined by fluorescence spectroscopy. Linear regression of data results in: $y = 98.65 x + 0.44$, $r^2 = 1$.

Osmolality Studies

To study the effect of atrazine and propylene glycol on the osmolality of atrazine containing solutions, three samples of 92.7 µM atrazine solutions were prepared by dissolving atrazine in KRB, KRB + propylene glycol (95:05) and KRB + propylene glycol (50:50). Solutions osmolality were measured by placing 10 µl of each sample into the measurement chamber of a pre-calibrated Wescor® 5500 vapor pressure osmometer (Wescor Inc., Logan, UT).

Histological Studies

Nasal mucosal olfactory and respiratory tissue sections were rinsed with KRB and then cut in 1cm² samples. Tissue samples were collected after the completion of the diffusion studies using KRB, 92.7 µM atrazine in KRB, 92.7 µM atrazine in KRB + propylene glycol (50:50) and 92.7 µM atrazine in KRB + propylene glycol (95:05). Each tissue sample was fixed in zinc formalin solution (10 mL) for 48 hours followed by treatment with 10%, 20% and 30% sucrose solutions each for 24 hours, successively. Tissues samples were cryo-frozen with tissue freezing media (TFM-C™) (Triangle Biomedical Science, Durham, NC) using liquid nitrogen and cooled to -20°C using a snap freezing system (Gentle Jane® Instrumedics Inc., Hackensack, NJ). Sections (10µm thick) were cut from the tissues using a Microm® Cryostat II (HM505E) with a CryoJane system (Microm International, Walldorf, Germany) at -35°C. The sections were placed on Surgipath® adhesive coated slides (CSFA-1X, Leica Biosystems Richmond Inc., Richmond, IL) and stained using hematoxylin and eosin at room temperature using a DRS-601 Sakura diversified stainer (Sakura Finetek Inc., Torrance, CA). Finally, the sections were cover slipped and examined using bright field microscopy with an Olympus BX-61 motorized light microscope (Olympus Microscope and Imagining System Inc., Melville, NY).

Artificial Membrane Transport Studies

Transport of atrazine across an artificial membrane was carried out by using PermeGear® Side-by-Side horizontal diffusion cells (PermeGear Inc., Hellertown, PA). The artificial membrane, Silastic® medical grade sheeting, (1.27 mm-thick) was obtained from Dow Corning

Medical (Midland, MI). The membrane was cut to the dimensions of the diffusion cells and mounted between the donor and receiver chambers. The diffusional cross sectional area of the membrane was 1.77cm^2 and the volume of each cell was 7 mL. The diffusion cells were maintained at the desired temperature (37° C) by circulating water through the outer jacket using a Lauda RM6 circulating water bath (Brinkmann Instruments Co, Westbury, NY). Atrazine dissolved in KRB or in KRB:PG (50:50) was placed on the donor side and the receiver side was replaced with same solution without atrazine. Samples (200 µL) were removed from the receiver chamber at regular time intervals up to 24 hours and were analyzed for the concentration of permeant by HPLC. The solution removed was replaced with fresh, pre-warmed receiver solution.

Statistical Analysis

GraphPad Prism 6.03 software (GraphPad Software Inc., San Diego, CA) was used for data analysis. Linear regression analysis was carried out 1) to determine the slope of the steady-state portion of each flux plot obtained during the transport studies; 2) to describe the increase in flux with increasing donor concentration for the transport of atrazine; 3) for the construction of the calibration curves for atrazine and LY, and solubility studies. The software was also used to construct the bar graphs of all the results obtained from the transport, LY, solubility and TEER studies.

CHAPTER 4

RESULTS AND DISCUSSION

Solubility Studies

The molar solubility of atrazine in KRB was determined to be 150.8 µM, whereas, in a mixture of KRB: propylene glycol (95:05), the solubility was 221.1 µM and in KRB: propylene glycol (50:50), the solubility was estimated to be 1529.6 µM at 25°C. Figure 4-1 shows the calculated solubility of atrazine in the three different solvents.

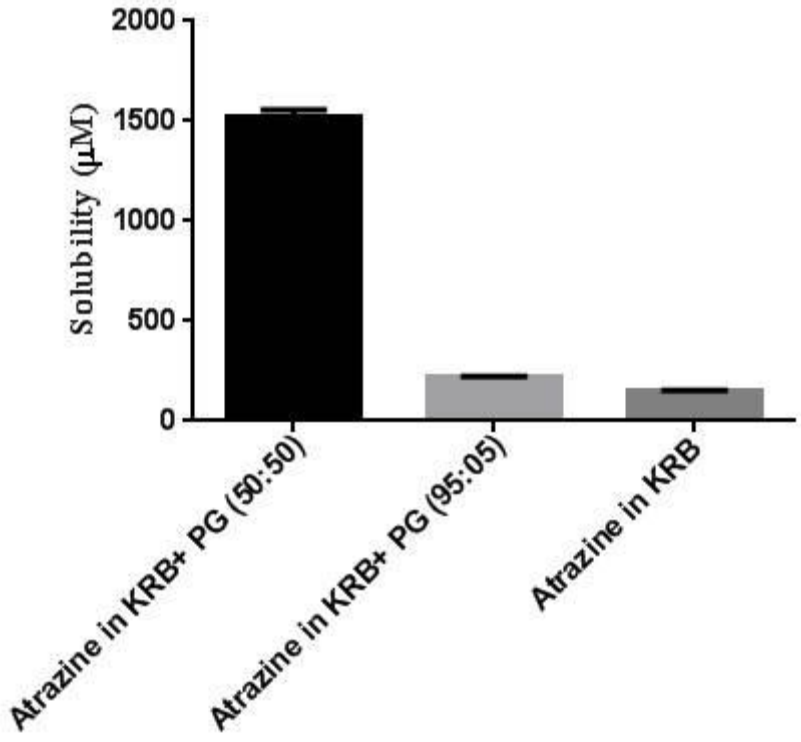

Figure 4-1 Comparison of atrazine solubility in mixtures of KRB and propylene glycol (PG). Results are expressed as the mean ± standard deviation of three measurements. The solubilities are statistically different between the three solutions (one-way ANOVA followed by Tukey's multiple comparison test, $p<0.005$).

Transport Studies

The flux of atrazine across respiratory and olfactory tissues was observed to increase in a linearly with increasing donor concentration. No saturation in the flux was observed over the concentration range tested (46.3- 139.1 µM). The highest atrazine donor concentration (139.1 µM) was limited by the solubility of atrazine in KRB (150.8 µM). The average flux values of atrazine across the respiratory and olfactory mucosae are presented in Figures 4-2 and 4-3.

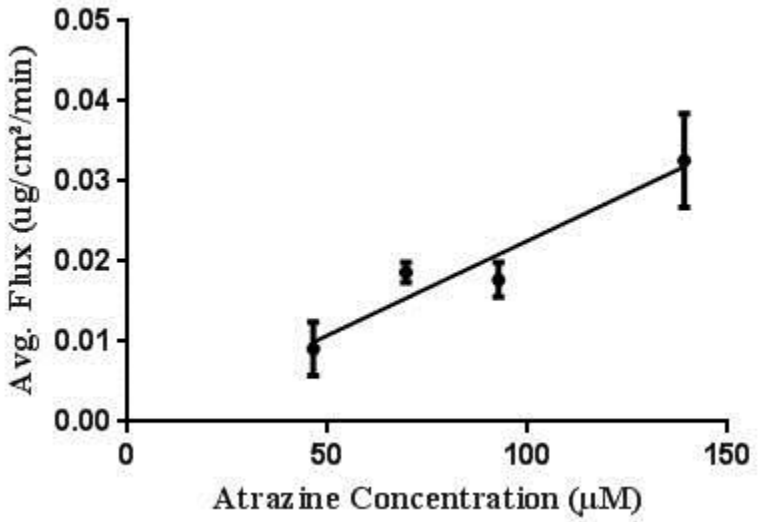

Figure 4-2 Concentration dependence of atrazine flux across bovine respiratory tissues in the mucosal to submucosal direction. Results are presented as the mean of 3 replicates ± standard deviation. Flux was calculated from transport studies carried out for 120 minutes. Linear regression of the flux data gave: $y = 0.00023x - 0.0007$, $r^2 = 0.92$.

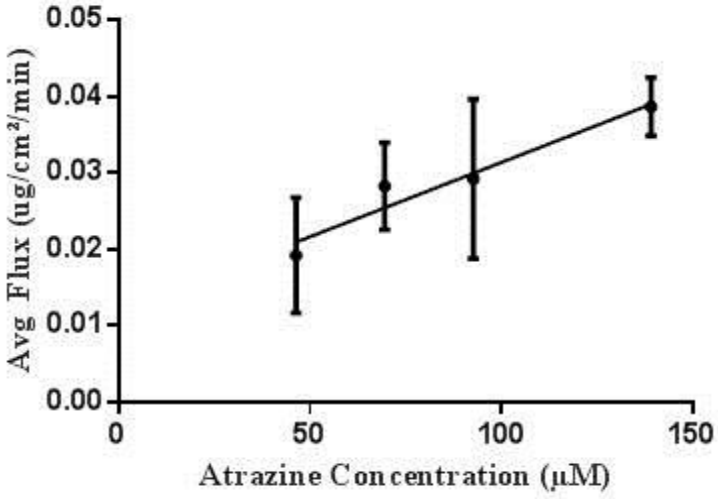

Figure 4-3 Concentration dependence of atrazine flux across bovine olfactory tissues in the mucosal to submucosal direction. Results are presented as the mean of 3 replicates ± standard deviation. Flux was calculated from transport studies carried out for 120 minutes. Linear regression of the flux data gave: $y = 0.00019x + 0.011$, $r^2 = 0.94$.

To compare the magnitude of atrazine flux across respiratory and olfactory tissues (Figure 4-4), the flux of atrazine across respiratory mucosae was scaled to the thickness of the olfactory mucosae which was reported to be equal to 0.4 mm for olfactory tissues and 0.75 mm for respiratory tissue[46], as shown in Equation 4-1. No differences between the tissues were noted except at the near saturated donor concentration of 139.1µM

$$(Respiratory\ thickness)\ /\ (Olfactory\ thickness) = 0.75\ mm/0.40\ mm = 1.8 \qquad \text{Equation 4-1(a)}$$

$$\frac{thickness\ normalized\ flux}{across\ respiratory\ mucosa} = flux\ across\ the\ respiratory\ mucosa\ \times 1.8 \qquad \text{Equation 4-1(b)}$$

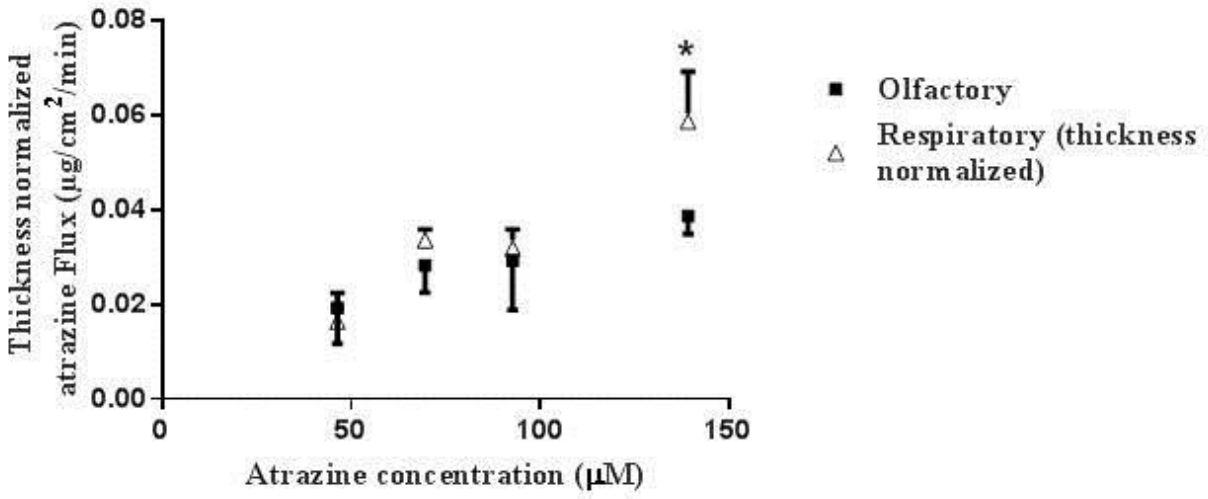

Figure 4-4 Comparison of thickness normalized flux of atrazine in KRB across bovine respiratory and olfactory tissues. Results are presented as the mean of three replicates ± standard deviation. Asterisk indicates a significant difference between the tissues ($p \leq 0.05$).

Inhibition Studies

At an atrazine concentration of 92.7 µM, no statistically significant differences in the flux of atrazine across the respiratory and olfactory tissues was observed when tissues were exposed to 2,4-DNP. Figures 4-5 and 4-6 compare the rate of atrazine flux across respiratory and olfactory tissues in the presence and absence of 2,4-DNP.

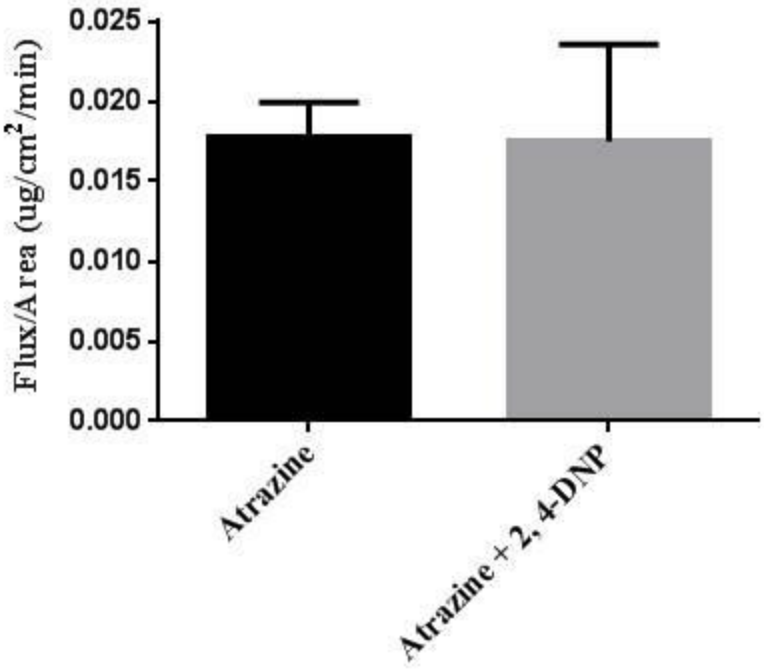

Figure 4-5 Comparison of atrazine (92.7 µM) flux across bovine respiratory tissues in the presence and absence of 2,4-DNP.

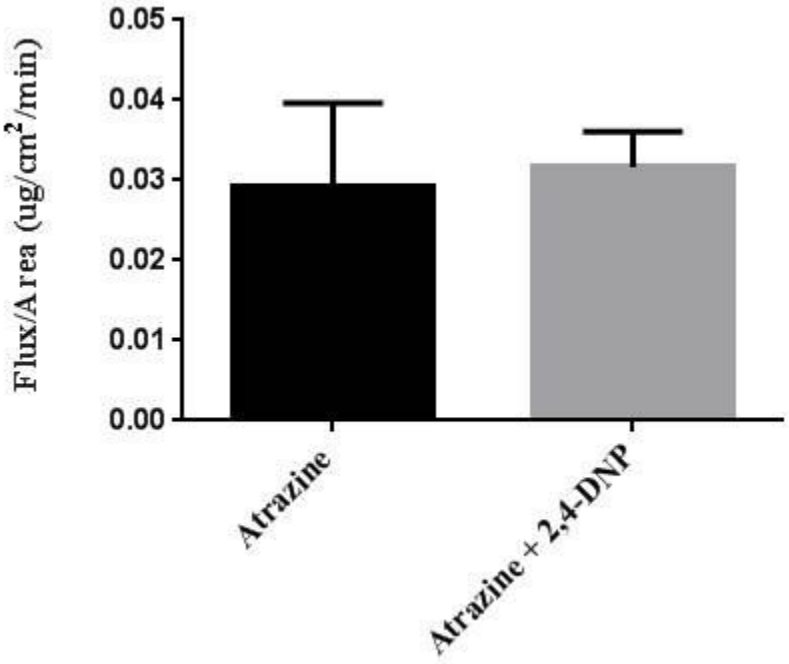

Figure 4-6 Comparison of atrazine (92.7 µM) flux across bovine olfactory tissues in the presence and absence of 2,4-DNP.

Co-solvent Studies

The flux of atrazine across respiratory tissues (Figure 4-7) when it was dissolved in a mixture of KRB: propylene glycol (95:05) was similar to the values obtained using KRB; however, a significant decrease in the flux of atrazine was observed when it was dissolved in KRB: propylene glycol (50:50).

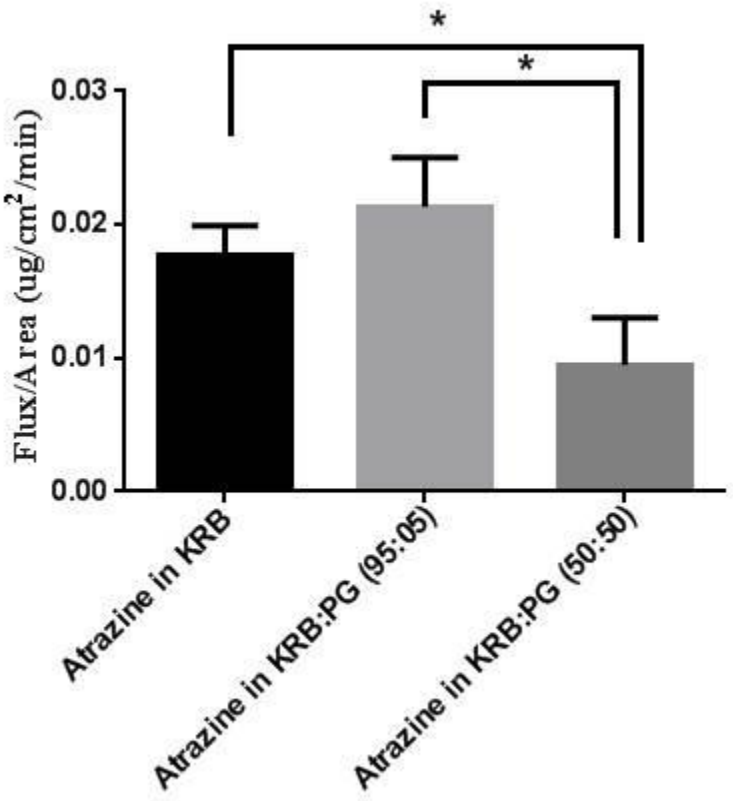

Figure 4-7 Comparison of atrazine (92.7 µM) flux across bovine respiratory tissues when atrazine was dissolved in mixtures of KRB and propylene glycol with different ratios. Asterisks indicate statistically significant differences between the measured values (one-way ANOVA followed by Tukey's multiple comparison test, $p \leq 0.05$).

For olfactory tissues (Figure 4-8), the flux of atrazine was not significantly different when atrazine was dissolved in KRB or a mixture of KRB: propylene glycol (95:05), yet the flux of atrazine significantly decreased compared to the 95:05 KRB: propylene glycol system when it was dissolved in a mixture of KRB: propylene glycol (50:50).

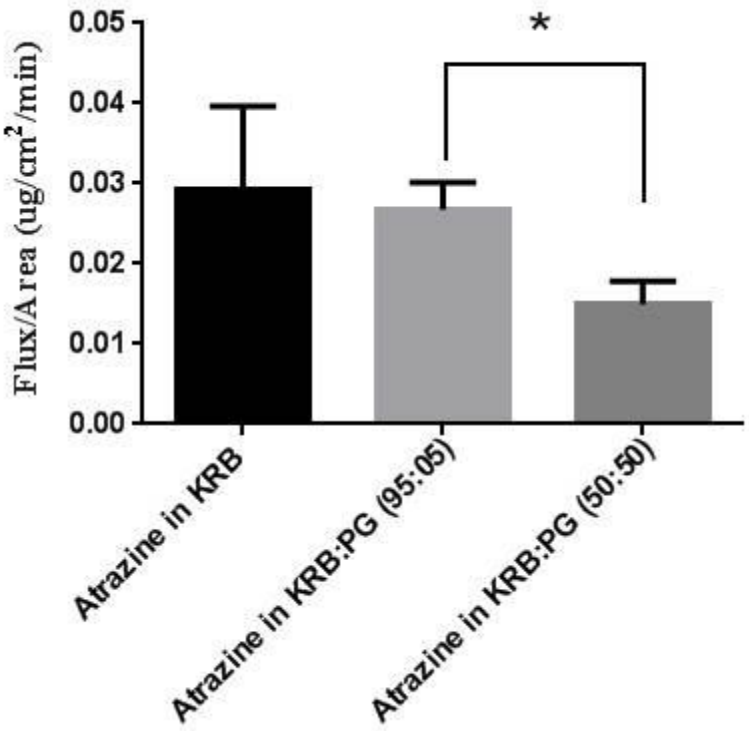

Figure 4-8 Comparison of atrazine flux across bovine olfactory tissues, when atrazine was dissolved in mixtures of KRB and propylene glycol. Asterisk indicates a significant difference between the measured values (one-way ANOVA followed by Tukey's multiple comparison test, $p<0.005$)

Silastic® Membrane Transport Studies

The flux of atrazine (92.7 µM) across a Silastic® silicone membranes was found to be higher than the flux of atrazine dissolved in a mixture of atrazine in KRB:PG (50:50) (Figure 4-9). Cumulative amount of atrazine in the receiver chamber versus time plot are presented in Appendix D.

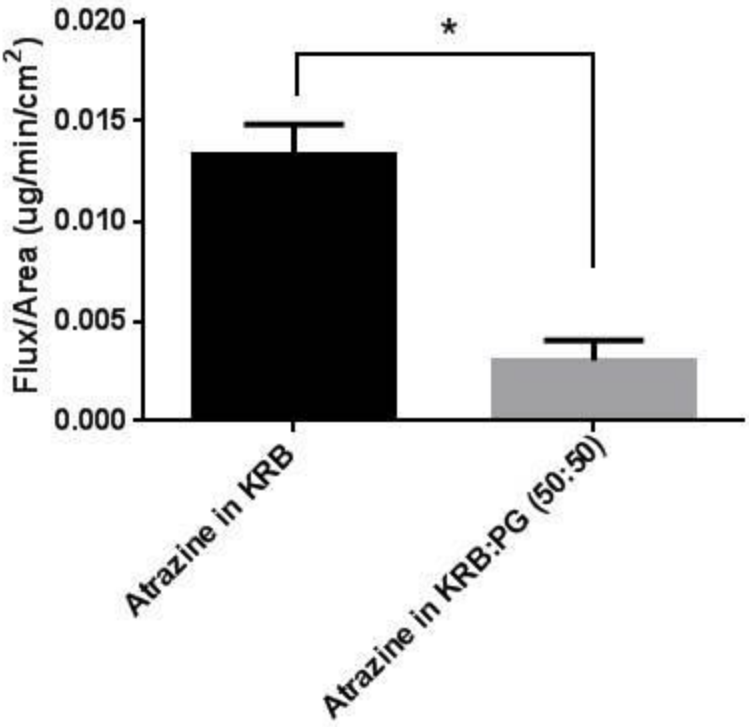

Figure 4- 9 Flux of atrazine in KRB and KRB:PG (50:50) across a Silastic® (0.05 inch thickness) membrane. Results are presented as the mean of 3 replicates ± standard deviation. Asterisk indicates a significant difference between the measured values (Student's t-test, $p \leq 0.05$).

Osmolality Studies

The osmolality of atrazine (92.7 µM) dissolved in KRB (250 mmol/kg ± 13.9) was not significantly different from the osmolality of KRB buffer solution used in the receiver chamber (255.2 mmol/kg ± 18.4). However, the osmolality of atrazine dissolved in KRB: propylene glycol mixture (95:05) was found to be 744.9 mmol/kg ± 1.8 which was slightly higher than the osmolality of the mixture of KRB: propylene glycol (95:05) without atrazine (719.3 mmol/kg ± 2.1) ($p=0.0062$). The osmolality values of atrazine dissolved in KRB: propylene glycol (50:50) and the osmolality of KRB: propylene glycol (50:50) mixture was higher than 1 mol/kg which was beyond the measurement range for the vapor pressure osmometer. Figure 4-10 presents the osmolality values obtained from the vapor pressure osmometer.

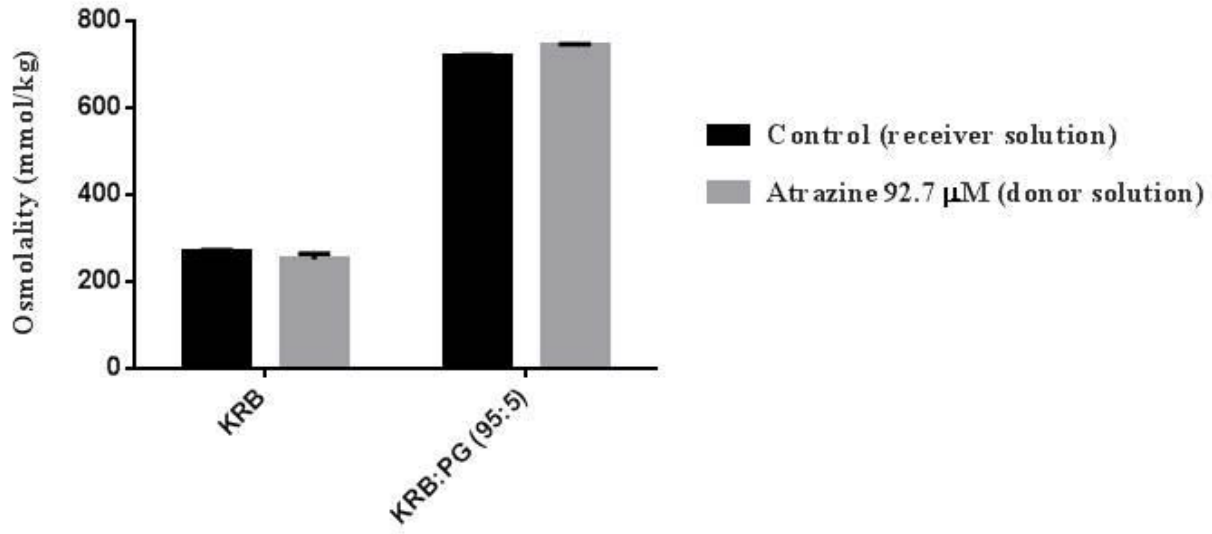

Figure 4-10 Osmolality values of KRB buffer and mixtures of KRB and propylene glycol (PG) (50:50) with and without atrazine. Osmolality was measured in mmol/kg, and each value represents the mean of 3 replicates ± standard deviations.

Tissue Viability Studies

Transepithelial electrical resistance (TEER) measurements were made before and after each study as well as at the initial time point during each study. TEER values above 100 Ω*cm^2 were considered to be indicative of intact mucosal explants. Average TEER values of transport studies are presented in Appendix B, and a representative bar graph of the TEER values across respiratory and olfactory tissues exposed to 92.7 µM atrazine dissolved in KRB are presented in Figures 4-11 and 4-12, respectively.

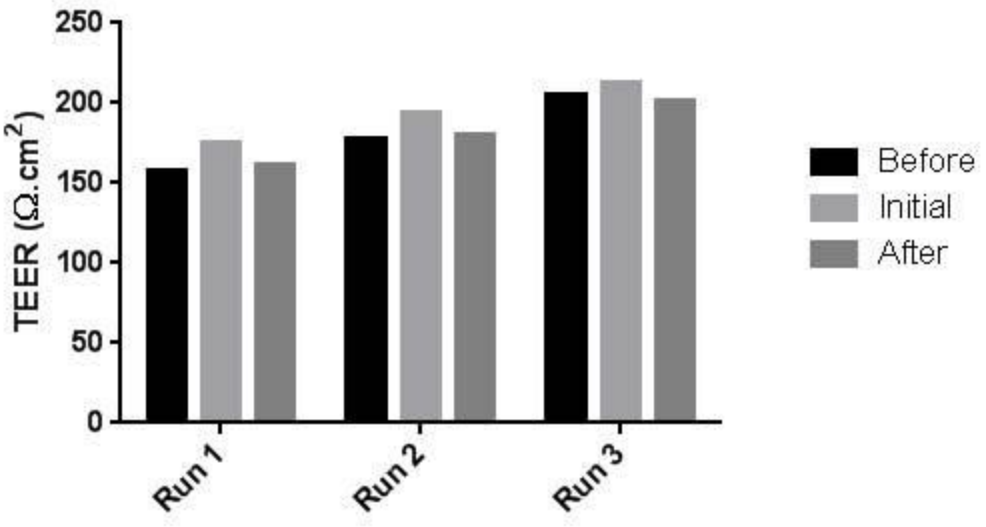

Figure 4-11 TEER values across respiratory tissues exposed to atrazine (92.7 uM) dissolved in KRB. The values are measured in Ω*cm^2. *"Before"* refers to the values taken before the equilibration of the diffusion cells before introducing atrazine into the donor chamber; "*initial"* refers to the values taken at the beginning of the transport experiment and "*after"* expresses the values measured at the end of the transport experiment.

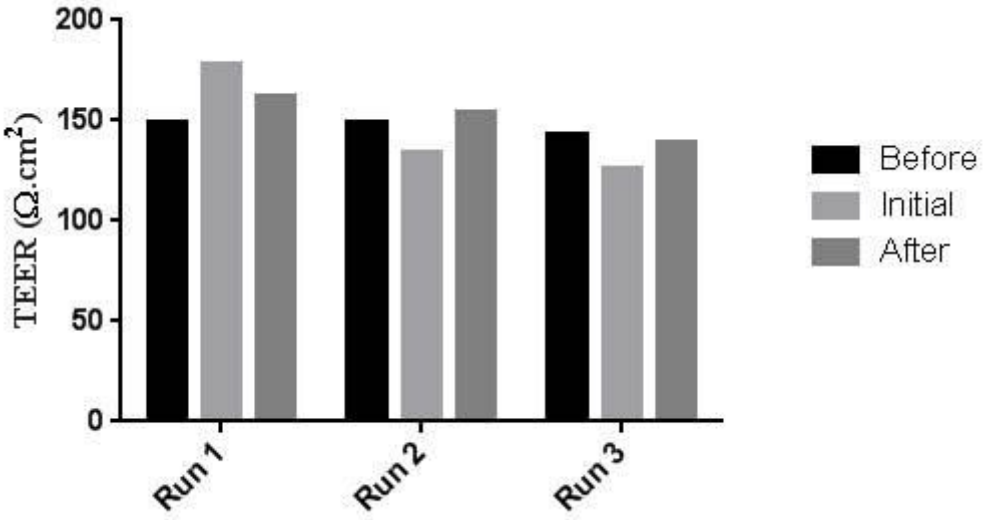

Figure 4-12 TEER values across olfactory tissues exposed to atrazine (92.7 uM) dissolved in KRB. The values are measured in $\Omega*cm^2$. "*Before"* refers to the values taken at the equilibration of the diffusion cells before introducing atrazine into the donor chamber; "*initial"* refers to the values taken at the beginning of the transport experiment and "*after"* expresses the values measured at the end of the transport experiment.

To assess the integrity of the tight junctions in the bovine respiratory and olfactory tissues, the transport of Lucifer Yellow a small hydrophilic marker compound, transported across the tissue explants was measured (Figures 4-13 and 4-14).

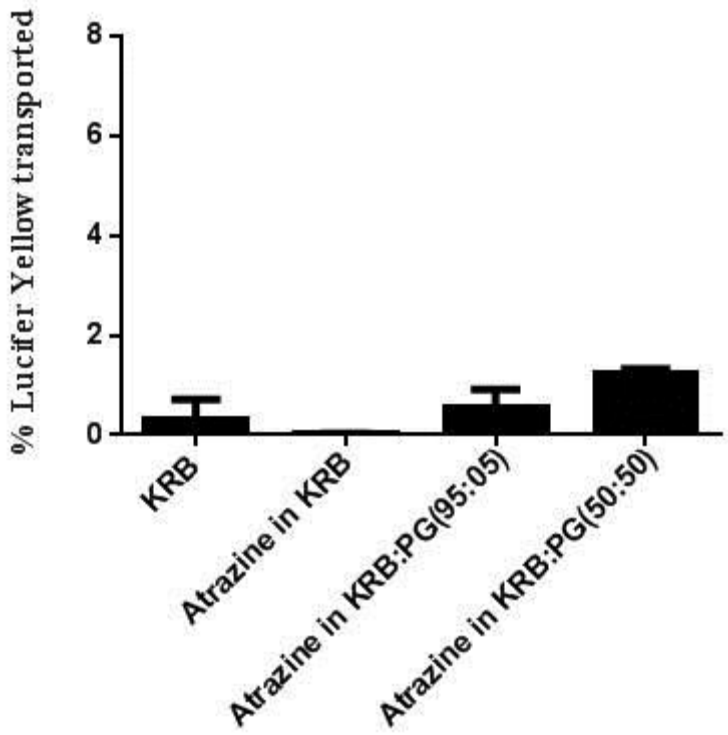

Figure 4-13 Percent transport of the paracellular marker Lucifer Yellow (100 µM) after one hour through respiratory tissues. KRB refers to tissues exposed to Lucifer Yellow after being exposed to KRB for two hours at 37°C and the remaining bars refer to tissues exposed to Lucifer Yellow after two hours of exposure to atrazine dissolved in KRB:PG at different ratios.

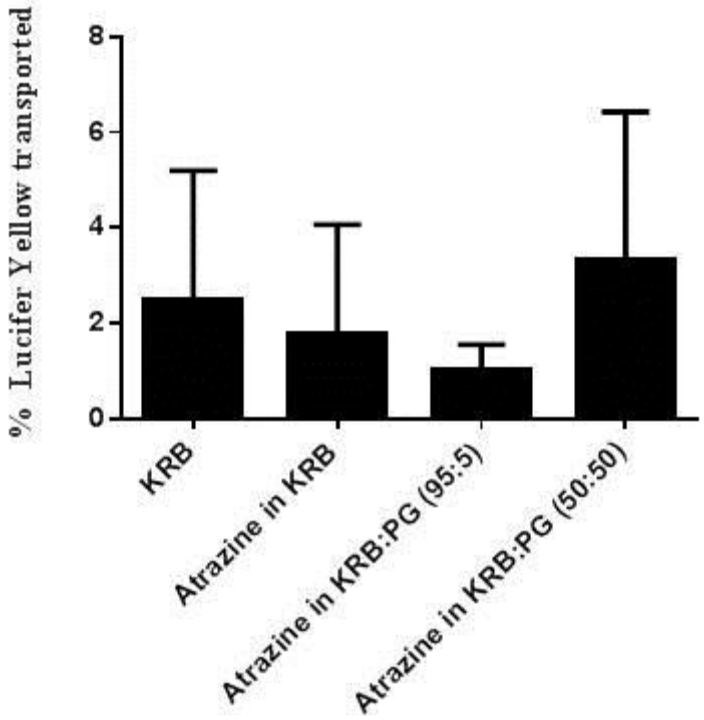

Figure 4-14 Percent transport of the paracellular marker Lucifer Yellow (100 µM) after one hour through olfactory tissues. KRB refer to tissues exposed to Lucifer Yellow after being exposed to KRB for two hours at 37°C and the remaining bars refer to tissue exposed to Lucifer Yellow after two of exposure to atrazine dissolved in KRB:PG with different ratios.

Histological Evaluation

Light microscopy shows that the olfactory tissues contain ciliated pseudostratified columnar epithelial cells covering a highly vascular and glandular lamina propria. The sub-mucosal layer is composed of blood vessels, lymphatic vessels and nasal glands surrounded by connective tissue (Figure 4-15). The respiratory tissues have the same structural composition as the olfactory mucosae with the exception of having goblet cells scattered within the ciliated epithelium and a more dense cellular lamina propria composed of blood vessels and serous glands embedded in connective tissues in the submucosal region (Figure 4-16).

Figure 4-15 Bright field microscopic image of a hematoxylin and eosin stained section of bovine olfactory mucosae (10 µm thickness). The bovine olfactory tissue consists of pseudostratified columnar epithelium overlying lamina propria (20X). *Abbreviations:* (A) basement membrane, (B) Bowman's gland, (C) blood vessels, (D) epithelial layer, and (E) submucosal region.

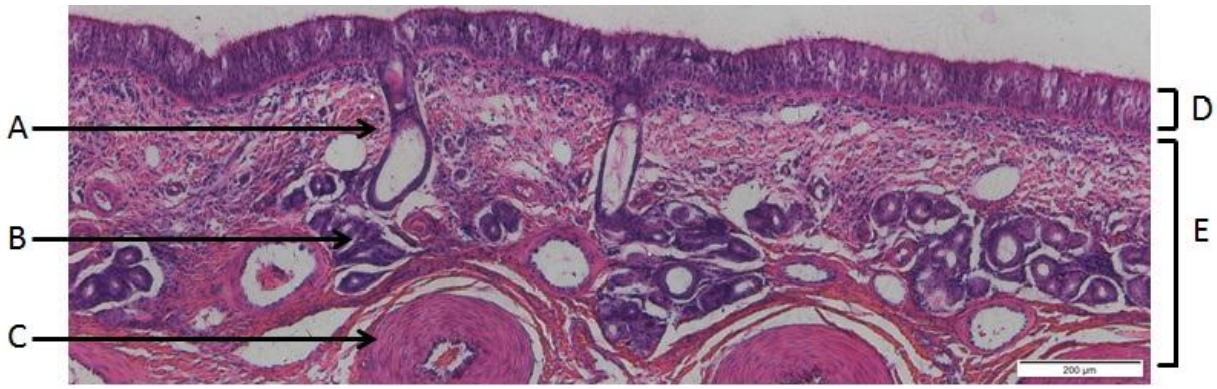

Figure 4-16 Bright field microscopic image of hematoxylin and eosin stained section of bovine respiratory mucosae (10 µm thickness). The bovine respiratory mucosa consists of pseudstratified columnar epithelium and an underlying lamina propria (20X). *Abbreviations:* (A) goblet cells, (B) serous glands, (C) blood vessels, (D) epithelial layer and (E) submucosal region.

In respiratory tissues, an erosive effect on some regions of the epithelium was observed following exposure to KRB (Figure 4-17). Atrazine showed an even greater erosive effect on the respiratory epithelium (Figure 4-18). For atrazine dissolved in a mixture of KRB and propylene glycol (95:05), the erosive effects on the epithelial cells were even more pronounced (Figure 4-19), and with atrazine dissolved in KRB:PG (50:50), histological examination showed complete removal of the epithelial layer from the apical side of the membrane (Figure 4-20).

Figure 4-17 Brightfield microscopic image of respiratory tissue exposed to KRB for two hours (20X). Tissue showed some patches of altered epithelium.

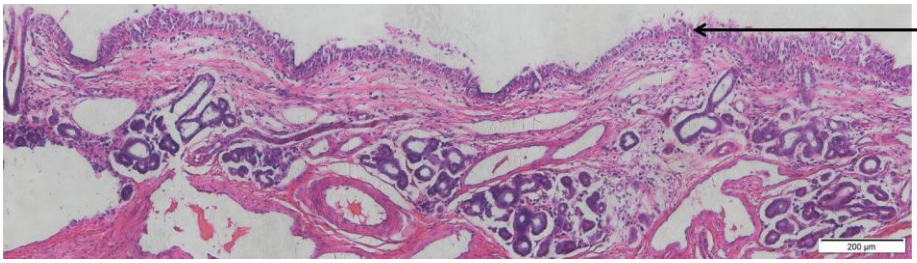

Figure 4-18 Effect of atrazine dissolved in KRB on the apical side of the respiratory epithelium (20X). Alterations of the epithelial layer were observed throughout the section.

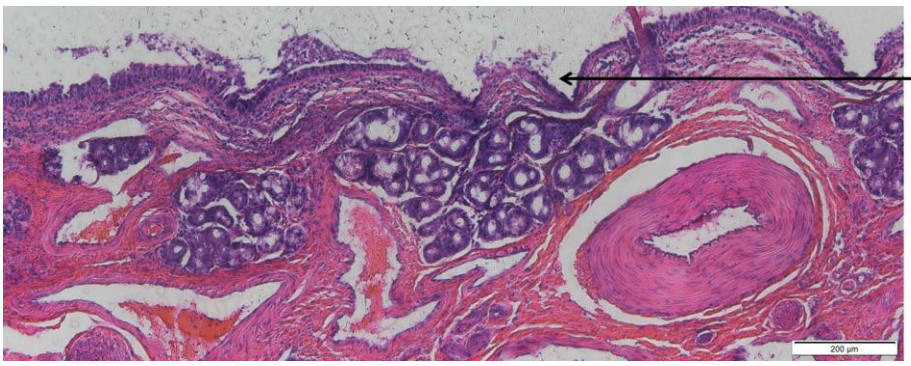

Figure 4-19 Effect of atrazine dissolved in KRB: propylene glycol (95:05) on the apical surface of the respiratory epithelium (20X). Atrazine solution produced considerable erosion of the epithelial layer.

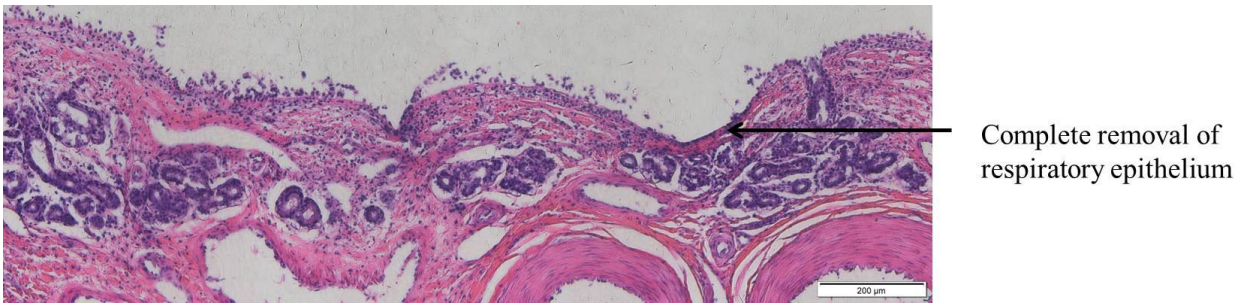

Figure 4-20 Effect of atrazine dissolved in KRB: propylene glycol (50:50) on the apical side of the respiratory epithelium (20X). Atrazine solution produced complete removal of the respiratory epithelium compared to control.

In the olfactory tissues, no change on the olfactory epithelium was observed when the tissue was exposed to KRB (Figure 4-21). A greater erosive effect was observed in tissue samples exposed to atrazine dissolved in KRB and mixture of KRB: propylene glycol (95:05), as shown in Figures 4-22 and 4-23, respectively.

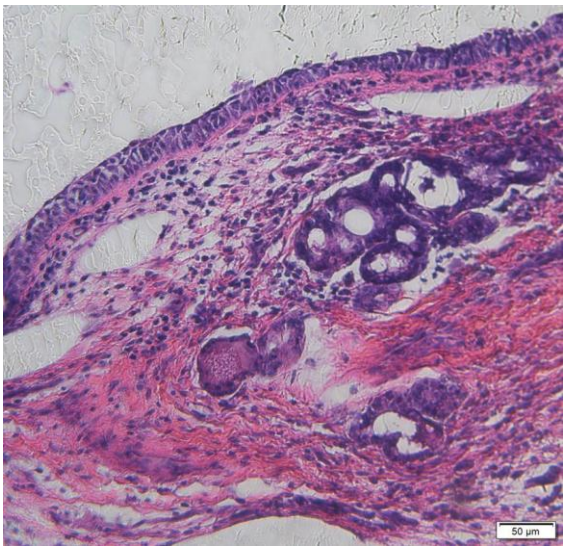

Figure 4-21 Brightfield microscopic image of olfactory tissues exposed to KRB for two hours (20X).

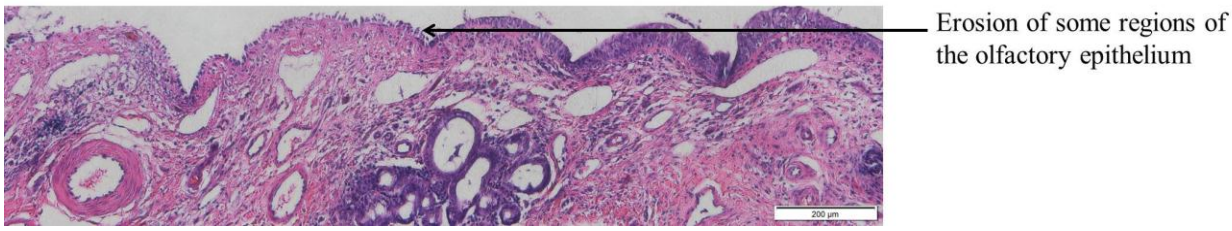

Figure 4-22 Effect of atrazine dissolved in KRB on the apical side of the olfactory epithelium (20X). Atrazine showed partial erosion of some regions of the olfactory epithelium compared to control.

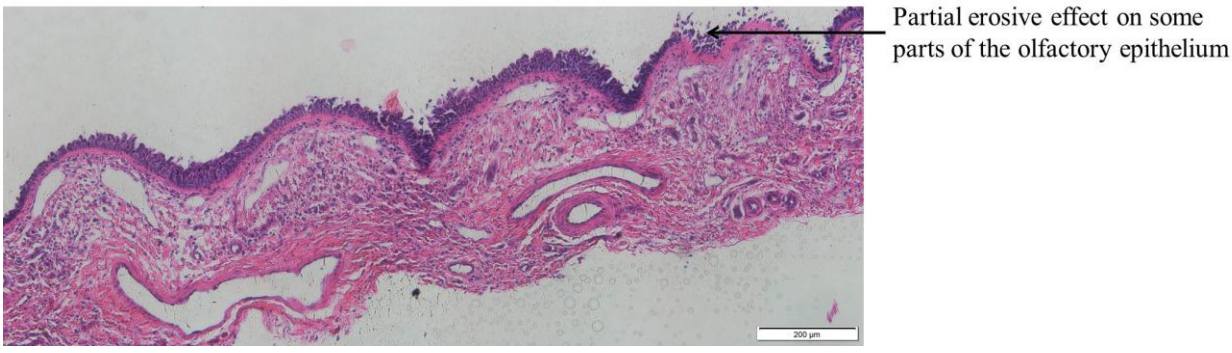

Figure 4-23 Effect of atrazine dissolved in KRB: propylene glycol (95:05) on the apical side of the olfactory epithelium (20X). Atrazine solution produced partial erosion of some regions of the olfactory epithelium compared to control.

Atrazine solution dissolved in KRB: propylene glycol (50:50) showed removal of most parts of the olfactory epithelium, as shown in Figure (4-24).

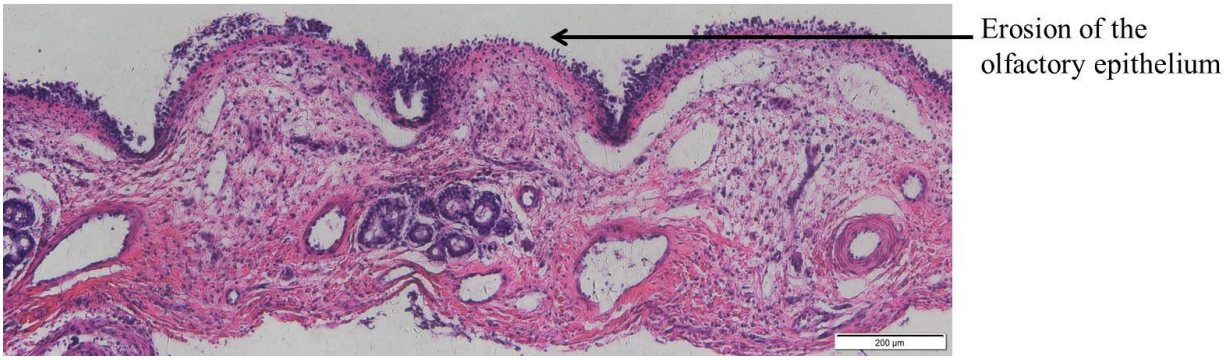

Figure 4-24 Effect of atrazine dissolved in KRB: propylene glycol (50:50) on the apical side of the olfactory epithelium (20X). Atrazine solution produced complete removal of the olfactory epithelium compared to the control.

Discussion

The observed concentration dependent transport and the absence of saturation suggest that atrazine was primarily transported across bovine nasal mucosae in a manner consistent with passive diffusion in the concentration range tested (46.3-139.1 µM). The higher average rate of atrazine flux across olfactory tissues compared to respiratory tissues may be attributed to the structural difference between the respiratory and olfactory tissues.

Atrazine uptake was probed using the metabolic inhibitor 2,4-DNP, a substance which inhibits ATP synthesis by interfering with oxidative phosphorylation. Thus, all ATP-dependent transport processes will be inhibited in its presence. For instance, ATP- powered transporters such as the ATP binding cassette (ABC) pumps, require ATP and use the energy provided by its dephosphorylation to drive the transport of various molecules, including inorganic ions, metals, peptides, sugars and many other small molecules across all cell membranes against their electrochemical gradient [47]. If atrazine uptake involves an energy dependent component, a change in flux would be expected to be observed. However, after the nasal tissues were exposed to 2,4-DNP, the average flux of atrazine was not significantly changed for either respiratory and olfactory mucosae.

Propylene glycol, which is known as an inexpensive, non-toxic and well tolerated co-solvent[48], was also tested for its effect on the flux of atrazine since it is commonly used in the commercial atrazine-containing products. The flux of atrazine in a mixture of KRB:PG (50:50) across olfactory tissues was interestingly found to be significantly lower than the flux of atrazine dissolved in KRB across the same tissue. For respiratory tissue, no difference was observed between the flux values of atrazine in KRB and mixtures of KRB:PG.

In order to characterize the flux of atrazine solution in a reproducible, well-characterized membrane and to eliminate tissue-associated variability, Silastic®, an inert silicone membrane which is a suitable model for evaluation of passive drug transport[49], was used. With the silicone membrane, atrazine dissolved in KRB:PG (50:50) was found to have a significantly lower flux than atrazine dissolved in KRB. This might be due to the fact that the permeability of atrazine in

KRB is higher than that of atrazine in KRB:PG (50:50) since the measured solubility of atrazine in KRB:PG (50:50) is more than ten times higher than the solubility of atrazine in KRB. This likely results in a lower partition coefficient for atrazine dissolved in KRB:PG (50:50) compared to atrazine in KRB. This reduced partioning results in a lower flux value (Equation 3-1).

In order to assess the integrity of the tight junctions between the epithelial cells, TEER values were measured. TEER measures the resistance to ion flux through the membrane. Since ions are charged, they may only pass through paracellular spaces or via ion channels or transporters embedded in the membrane. Therefore, a high resistance to ion flow indicates significant tight junction formation. TEER values did not change significantly in tissue explants exposed to atrazine in KRB in the presence or absence of 2,4-DNP suggesting that atrazine does not cause any change to the integrity of tissue explants. TEER measurements are not relevant for tissue samples exposed to atrazine dissolved in (KRB:PG) mixtures since the EVOM^2 requires the use of a conductive liquid to give accurate measurements.

The high flux of Lucifer Yellow across the nasal epithelium is attributed to the use of water as a solvent in the transport experiment instead of KRB. The hypotonic donor solution likely increased water transport into the explant which resulted in increased Lucifer Yellow transfer due to osmotic changes to the membrane or due to "solvent drag effect" [50]. Previous investigators have shown in transport studies across the nasal epithelium that, flux of high molecular weight hydrophilic compounds like Lucifer Yellow is increased with the use of hypotonic solvents like water instead of isotonic vehicles[51].

Histological examination of the tissue explants using hematoxylin and eosin staining revealed that atrazine alone (92.7 μM), when compared to KRB controls, does not cause any significant morphological alterations to the nasal tissues. However, an alteration of the mucosal epithelium was observed for atrazine solutions containing PG. These results are not surprising since previous studies have shown that inhalation of 10% propylene glycol solution by rabbits for 20 minutes resulted in an alteration of the ciliated epithelium and an increase of mucus secretion by the goblet cells. It has also been observed that these effects were even more

pronounced with increasing duration of exposure[52]. These effects of PG on the nasal epithelium may play a role in the potential enhanced neurotoxicity of atrazine through direct nose to brain transport, especially since the commercial atrazine formulations also contain compounds in addition to PG, all of which may have a direct effect on the enhanced penetration and subsequent toxicity of inhaled atrazine.

Conclusions

Inhalation exposure of pesticides through the nasal cavity is one of the major pathways by which inhaled toxicants can reach the CNS directly, bypassing the blood-brain barrier. Many small molecules have shown a preferential uptake into the brain following intranasal administration; however, the mechanism of nose to brain transport is not fully elucidated and, furthermore, there are a limited number of studies investigating the CNS toxicity of chemicals following nasal inhalation.

Atrazine, a herbicide which is applied to crops to kill weeds, was banned in Europe in 2005 due to concerns of ground and drinking water contamination. Meanwhile, in the United State, more than 70 million pounds of atrazine are still applied to crops annually[20]. Recently, there have been a number of studies investigating the etiology of Parkinson's disease (PD), and dopaminergic toxicity associated with atrazine in addition to the reported case studies of patients having Parkinson's disease-like symptoms in areas exposed to atrazine strongly suggests a link between atrazine exposure and the occurrence of PD.

The investigation of the transport systems available to atrazine showed that simple passive diffusion is the primary mechanism of atrazine flux across nasal mucosal tissues. The results also suggest that atrazine is not likely to be a substrate of energy dependent transporters in the nasal epithelium. Atrazine molecules, by themselves, do not cause any significant change in the mucosal epithelium, but the adjuvant compounds included in the commercial atrazine products to enhance solubility of atrazine, propylene glycol in particular, disrupt the epithelial barrier of the mucosal tissues which in turn may enhance atrazine penetration.

This highlights the fact that the resulted toxicity of atrazine may not only be related to its unpreventable contamination of drinking water but, instead, may also due to the inhalation of sprayed atrazine products by people working and residing nearby exposed areas.

APPENDIX A

COMPOSITION OF KREB'S RINGER BUFFER (KRB)

Salt	**Concentration (mM)**
$MgCl_2.6\ H_2O$	1.67
KCl	4.56
NaCl	119.78
$NaH_2PO_4 \cdot H_2O$	1.5
Na_2HPO_4	0.83
D-glucose	10
$NaHCO_3$	15
$CaCl_2 \cdot 2H_2O$	1.2

APPENDIX B

MEAN TEER VALUES

Tissue Type	Atrazine in KRB exposed tissue (Ω*cm^2) (mean ± standard deviation)	Atrazine and 2,4-DNP in KRB exposed tissue (Ω*cm^2) (mean ± standard deviation)
Respiratory tissue	164.31 ± 13.8	187.8 ± 15.8
Olfactory tissue	168.9 ± 21.9	144.3 ± 11.9

Tissue Type	Atrazine in KRB:PG (50:50) exposed tissue (Ω*cm^2) (mean ± standard deviation)	Atrazine in KRB:PG (95:05) exposed tissue (Ω*cm^2) (mean ± standard deviation)
Respiratory tissue	1083.5 ± 82.1	177.1 ± 17.8
Olfactory tissue	957 ± 171.5	170 ± 13.6

APPENDIX C

ATRAZINE TRANSPORT DATA

The flux values of atrazine presented in Figures 4-2 and 4-3 were calculated from these plots. The concentration of atrazine listed in the title of each plot denotes the donor concentration. The regression equation for each line is given in the right column.

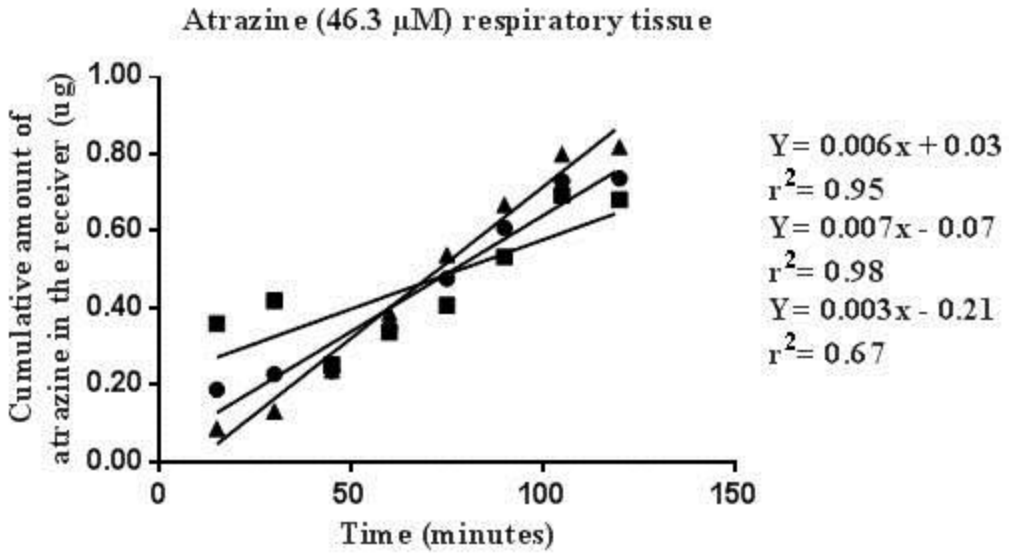

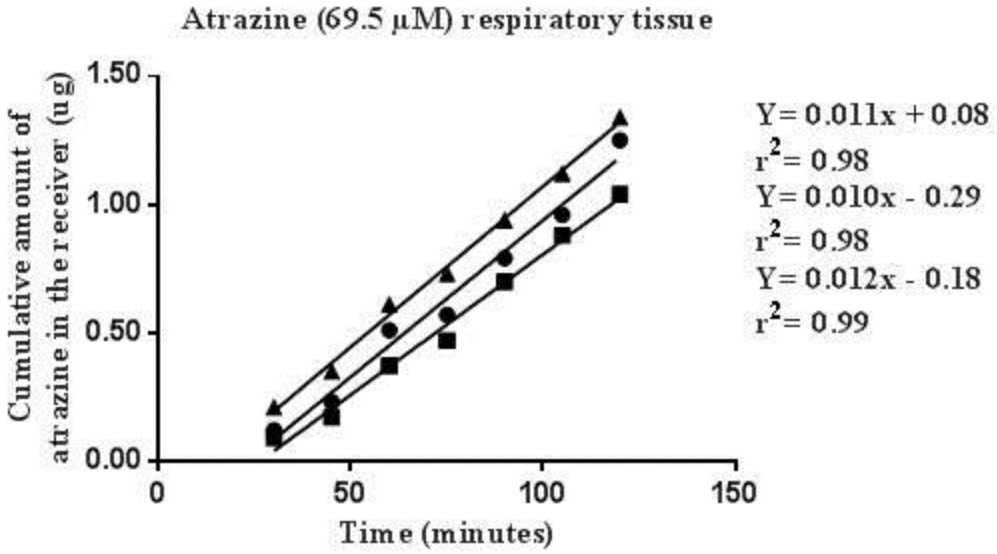
Atrazine (69.5 µM) respiratory tissue
Cumulative amount of atrazine in the receiver (ug)
1.50
1.00
0.50
0.00
0
50
100
150
Time (minutes)
Y= 0.011x + 0.08
r2= 0.98
Y= 0.010x - 0.29
r2= 0.98
Y= 0.012x - 0.18
r2= 0.99

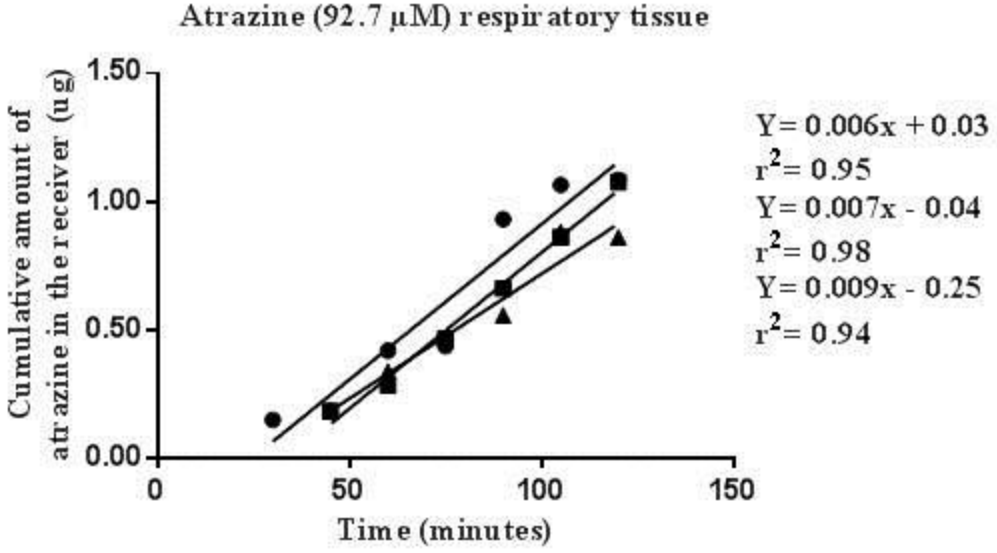
Atrazine (92.7 µM) respiratory tissue
Cumulative amount of atrazine in the receiver (ug)
1.50
1.00
0.50
0.00
0
50
100
150
Time (minutes)
Y= 0.006x + 0.03
r2= 0.95
Y= 0.007x - 0.04
r2= 0.98
Y= 0.009x - 0.25
r2= 0.94

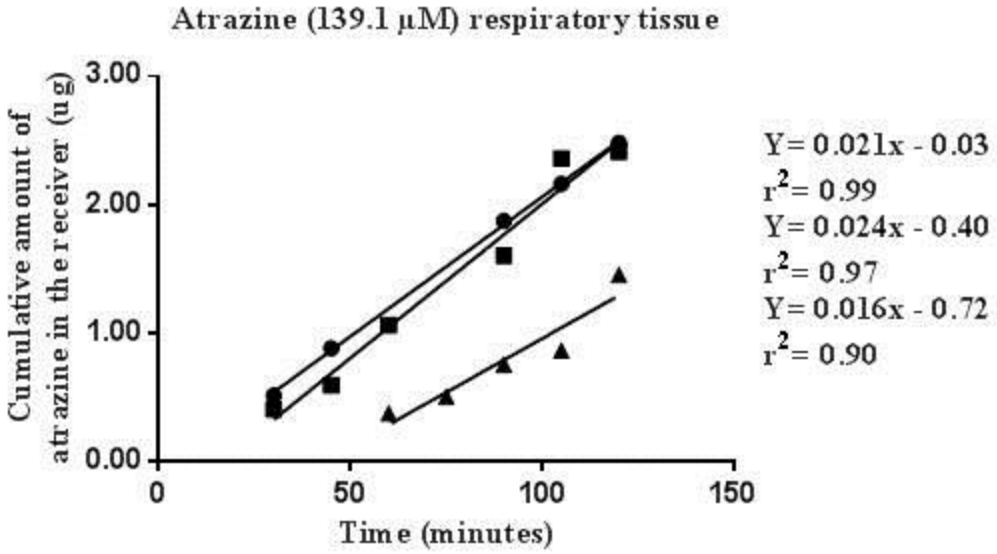
Atrazine (139.1 µM) respiratory tissue
Cumulative amount of atrazine in the receiver (ug)
3.00
2.00
1.00
0.00
0
50
100
150
Time (minutes)
Y= 0.021x - 0.03
r2= 0.99
Y= 0.024x - 0.40
r2= 0.97
Y= 0.016x - 0.72
r2= 0.90

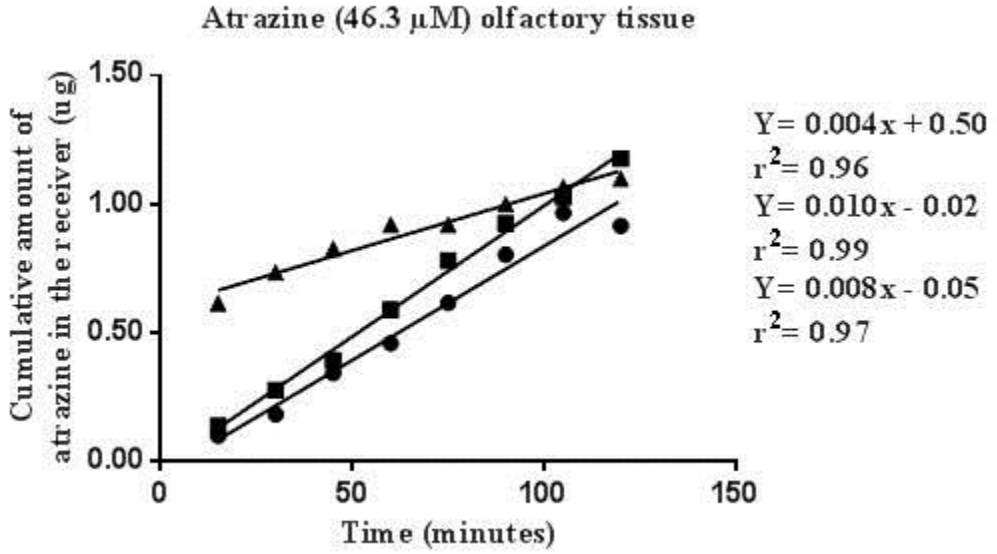
Atrazine (46.3 µM) olfactory tissue
Cumulative amount of atrazine in the receiver (ug)
1.50
1.00
0.50
0.00
0
50
100
150
Time (minutes)
Y= 0.004x + 0.50
r2= 0.96
Y= 0.010x - 0.02
r2= 0.99
Y= 0.008x - 0.05
r2= 0.97

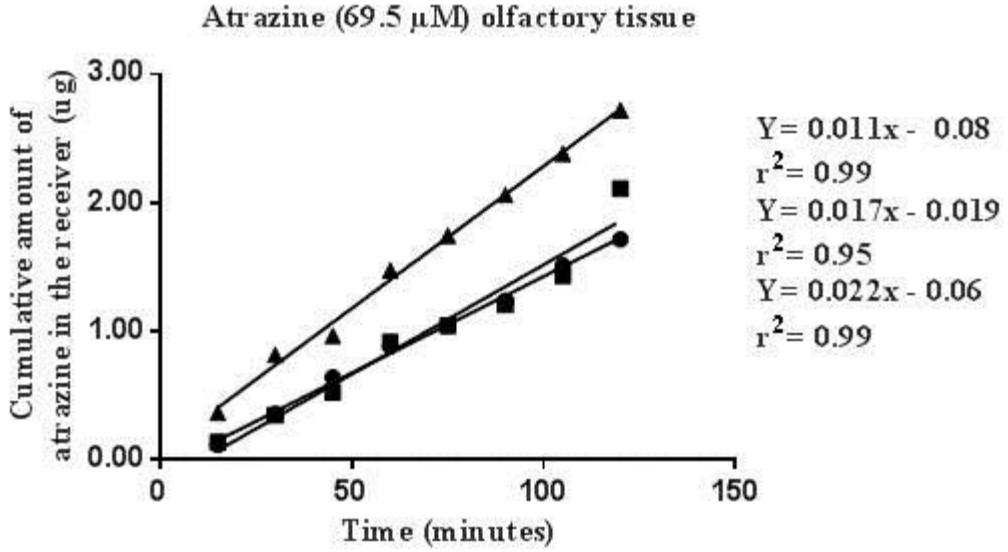
Atrazine (69.5 µM) olfactory tissue
Cumulative amount of atrazine in the receiver (ug)
3.00
2.00
1.00
0.00
0
50
100
150
Time (minutes)
Y= 0.011x - 0.08
r2= 0.99
Y= 0.017x - 0.019
r2= 0.95
Y= 0.022x - 0.06
r2= 0.99

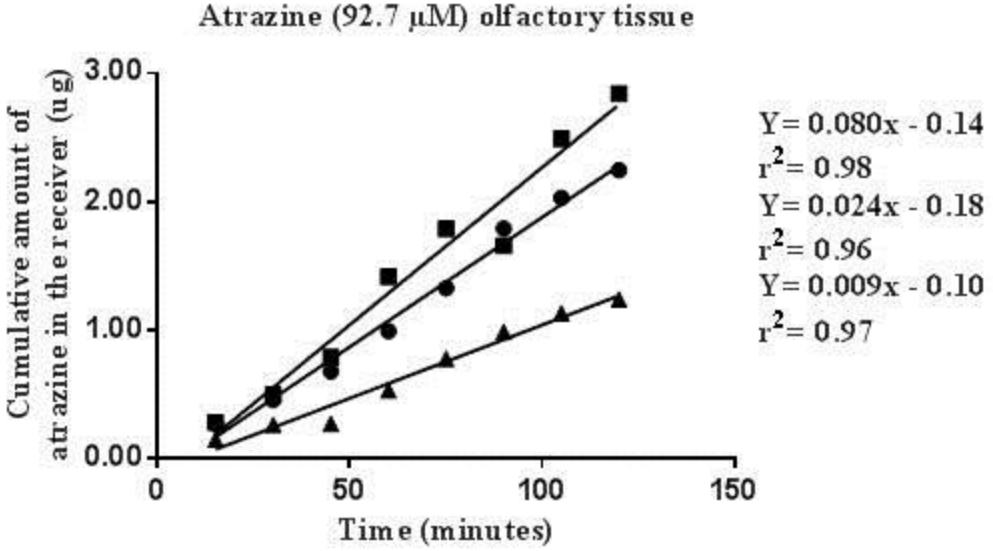
Atrazine (92.7 µM) olfactory tissue
Cumulative amount of atrazine in the receiver (ug)
3.00
2.00
1.00
0.00
0
50
100
150
Time (minutes)
Y= 0.080x - 0.14
r2= 0.98
Y= 0.024x - 0.18
r2= 0.96
Y= 0.009x - 0.10
r2= 0.97

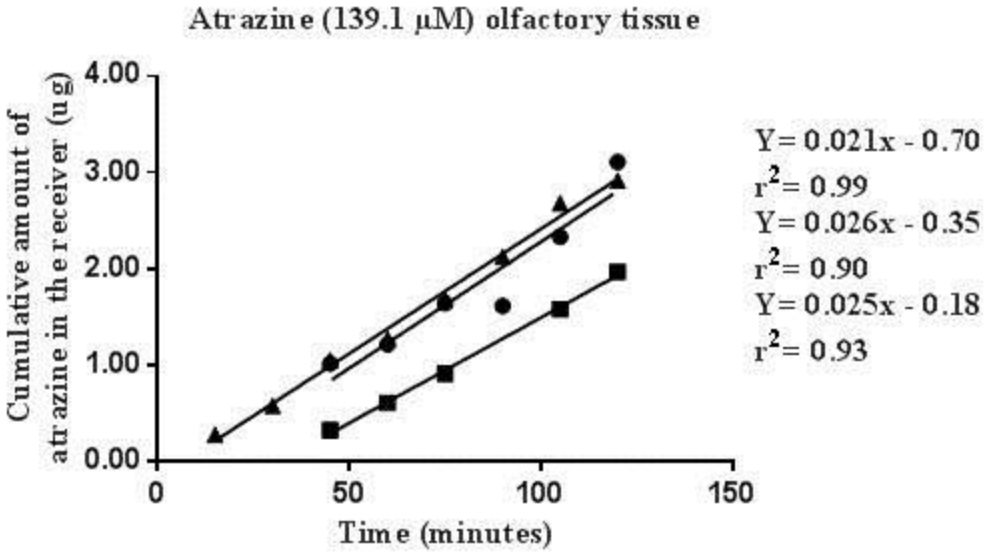
Atrazine (139.1 µM) olfactory tissue
Cumulative amount of atrazine in the receiver (ug)
4.00
3.00
2.00
1.00
0.00
0
50
100
150
Time (minutes)
Y= 0.021x - 0.70
r2= 0.99
Y= 0.026x - 0.35
r2= 0.90
Y= 0.025x - 0.18
r2= 0.93

APPENDIX D

SILASTIC® MEMBRANE TRANSPORT DATA

The flux values of atrazine presented in Figure 4-9 were calculated from these plots. The concentration of atrazine (92.7µM) listed in the title of each plot denotes the donor concentration. The regression equation for each line is given in the right column.

Abbreviations:

KRB: Krebs's Ringer's buffer.

PG: Propylene glycol.

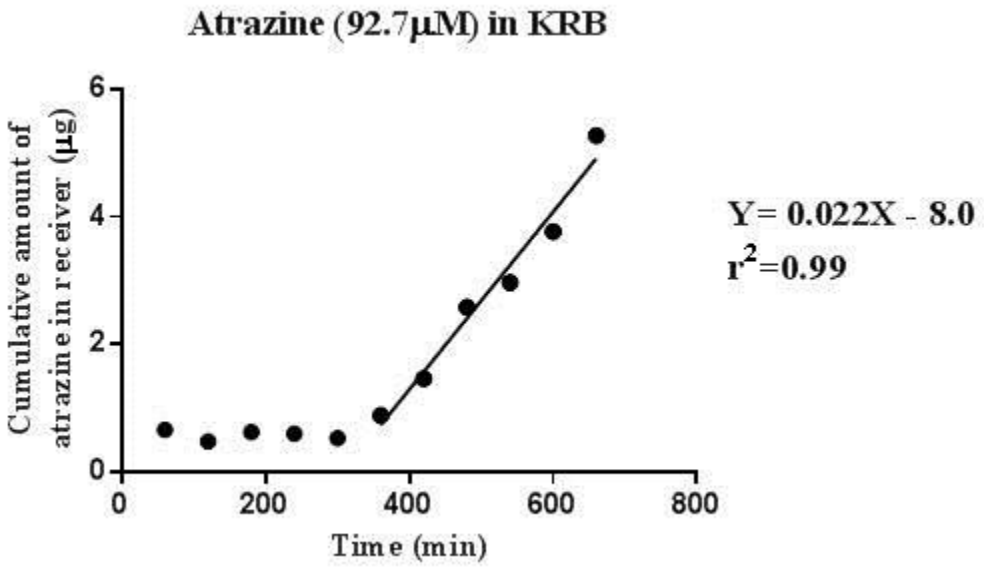

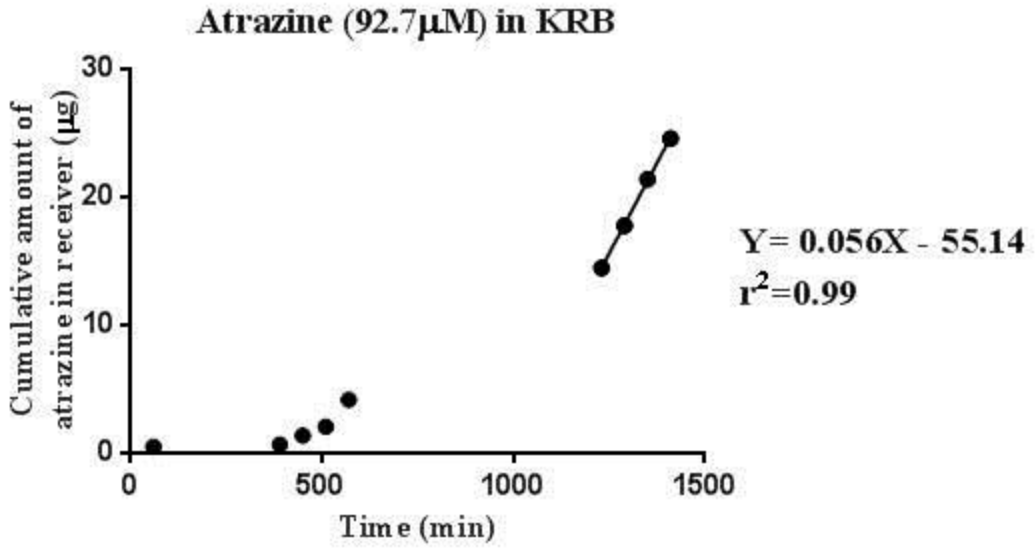
Atrazine (92.7µM) in KRB
Cumulative amount of atrazine in receiver (µg)
30
20
10
0
0
500
1000
1500
Time (min)
Y= 0.056X - 55.14
r2=0.99

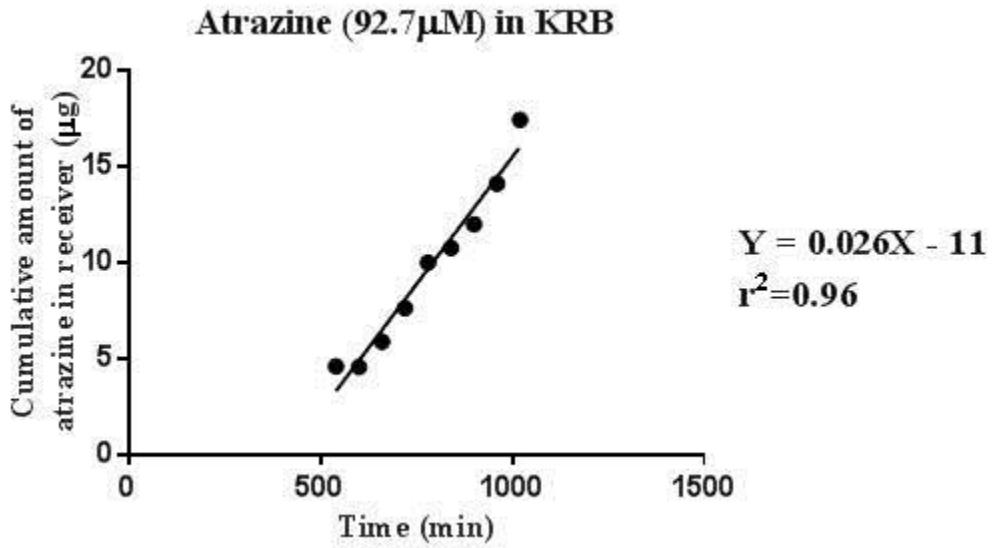
Atrazine (92.7µM) in KRB
Cumulative amount of atrazine in receiver (µg)
20
15
10
5
0
0
500
1000
1500
Time (min)
Y = 0.026X - 11
r2=0.96

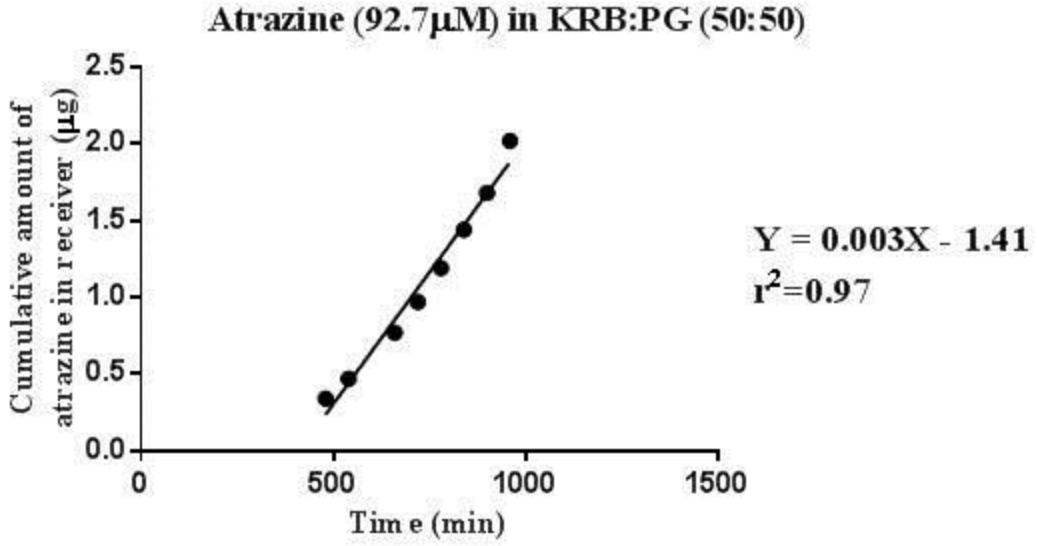
Atrazine (92.7µM) in KRB:PG (50:50)
Cumulative amount of atrazine in receiver (µg)
2.5
2.0
1.5
1.0
0.5
0.0
0
500
1000
1500
Time (min)
Y = 0.003X - 1.41
r2=0.97

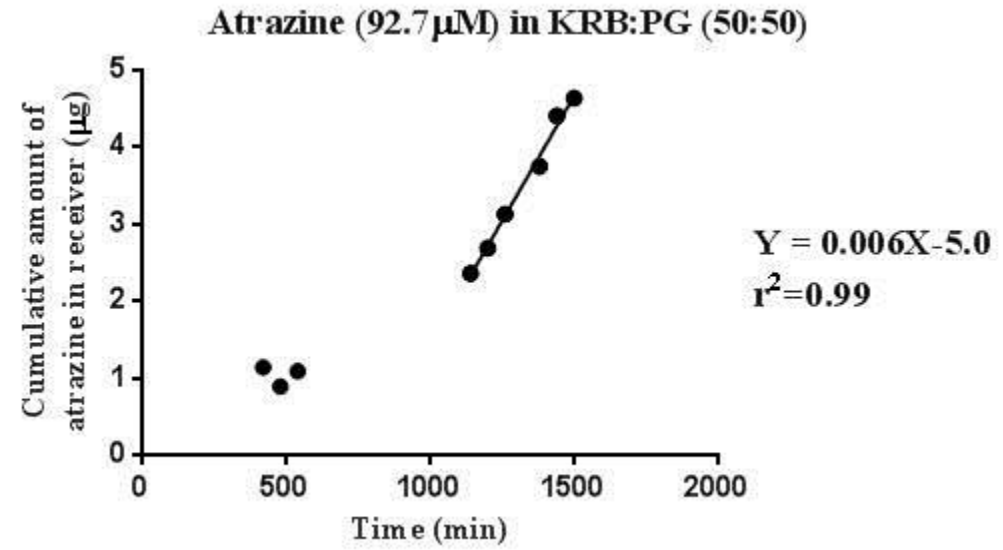
Atrazine (92.7µM) in KRB:PG (50:50)
Cumulative amount of atrazine in receiver (µg)
5
4
3
2
1
0
0
500
1000
1500
2000
Time (min)
Y = 0.006X-5.0
r2=0.99

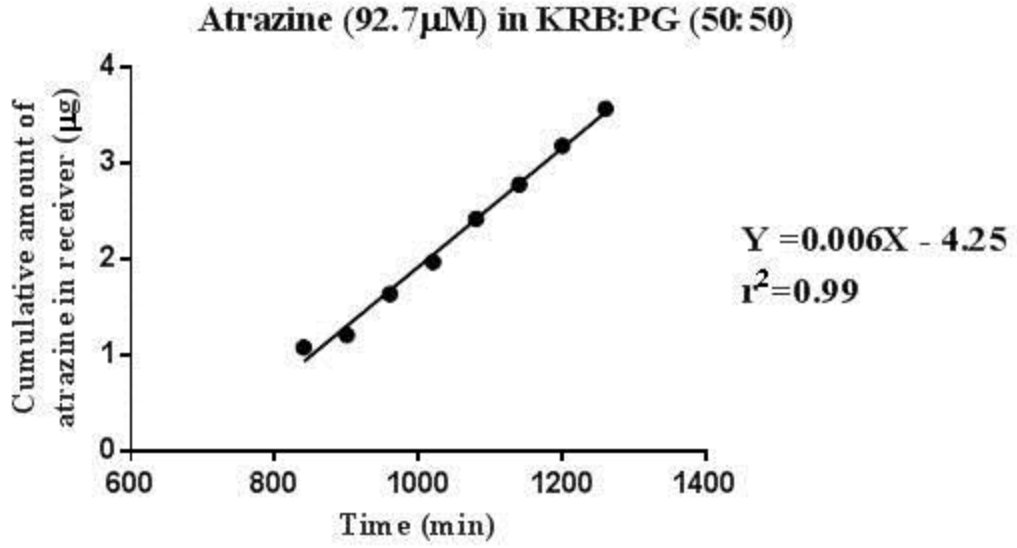
Atrazine (92.7µM) in KRB:PG (50:50)
Cumulative amount of atrazine in receiver (µg)
0
1
2
3
4
600
800
1000
1200
1400
Time (min)
Y =0.006X - 4.25
r2=0.99

REFERENCES

1. Weisenburger, D. D. Human health effects of agrichemical use. *Human Pathology* **24,** 571–6 (1993).

2. Ugwoke, M. I., Verbeke, N. & Kinget, R. The biopharmaceutical aspects of nasal mucoadhesive drug delivery. *The Journal of Pharmacy and Pharmacology* **53,** 3–21 (2001).

3. LeBaron M. The triazine herbicides: a milestone in the development of weed control technology. In *The Triazine Herbicide*, **1**; McFarland E., Burnside Orvin C.; Elsevier, San Diego, 2008.

4. Kligerman, A. D., Doerr, C. L., Tennant, A. H. & Zucker, R. M. Cytogenetic studies of three triazine herbicides. *Mutation Research/Genetic Toxicology and Environmental Mutagenesis* **465,** 53–59 (2000).

5. Sass, J. B. & Colangelo, A. European Union bans atrazine, while the United States negotiates continued use. *International Journal of Occupational and Environmental Health* **12,** 260–7 (2003).

6. Cooper, R. L. Lawes, S. C. Das, P. C. Nartosky, M. G. Goldman, J. M. Tyrey, E. L. & Stoker T. E. Atrazine and reproductive function: mode and mechanism of action studies. *Birth Defects Research. Part B, Developmental and Reproductive Toxicology* **80,** 98–112 (2007).

7. U.S. Environmental Protection Agency. *Atrazine, chemical summary*. 1–12 (2007). at <http://www.epa.gov/teach/chem_summ/Atrazine_summary.pdf>

8. National Center for Biotechnology Information. Atrazine. Pubchem Compound Database; CID=2256. (2014). at <http://pubchem.ncbi.nlm.nih.gov/summary/summary.cgi?sid=14708974&viewopt=PubChem#x395>

9. Shimabukuro, R. H. & Swanson, H. R. Atrazine metabolism, selectivity, and mode of action. *Journal of Agricultural and Food Chemistry* **17,** 199–205 (1969).

10. Adams, N. H., Levi, P. E. & Hodgson, E. In vitro studies of the metabolism of atrazine, simazine, and terbutryn in several vertebrate species. *Journal of Agricultural and Food Chemistry* **38,** 1411–1417 (1990).

11. Hanioka, N., Jinno, H., Tanaka-Kagawa, T., Nishimura, T. & Ando, M. In vitro metabolism of simazine, atrazine and propazine by hepatic cytochrome P450 enzymes of rat, mouse and guinea pig, and oestrogenic activity of chlorotriazines and their main metabolites. *Xenobiotica* **29,** 1213–26 (1999).

12. Guddewar, M. B. & Dauterman, W. C. Studies on a glutathione S-transferase preparation from mouse liver which conjugates chloro-s-triazine herbicides. *Pesticide Biochemistry and Physiology* **12,** 1–9 (1979).

13. Joo, H., Choi, K. & Hodgson, E. Human metabolism of atrazine. *Pesticide Biochemistry and Physiology* **98,** 73–79 (2010).

14. Ross, M. K., Jones, T. L. & Filipov, N. M. Disposition of the herbicide 2-chloro-4-(ethylamino)-6-(isopropylamino)-s-triazine (Atrazine) and its major metabolites in mice: a liquid chromatography/mass spectrometry analysis of urine, plasma, and tissue levels. *Drug Metabolism and Disposition: The Biological Fate of Chemicals* **37,** 776–86 (2009).

15. Lang, D. H., Rettie, a E. & Böcker, R. H. Identification of enzymes involved in the metabolism of atrazine, terbuthylazine, ametryne, and terbutryne in human liver microsomes. *Chemical Research in Toxicology* **10,** 1037–44 (1997).

16. Sarkar, M. A. Drug metabolism in the nasal mucosa. *Pharmaceutical Research* **9,** 1–9 (1992).

17. Cragin, L. A., Kesner, J. S., Bachand, A. M., Barr, B. B, Meadows, J. W., Kreig, E. F., and Reif J. S. Menstrual cycle characteristics and reproductive hormone levels in women exposed to atrazine in drinking water. *Environmental Research* **111,** 1293–301 (2011).

18. Hayes, T. B., khoury, V., Narayan, A., Nazir, M., Park, A., Brown, T., Adame, L., Chan, E., Buchholz, D., Stueve, T., and Gallipeau S. Atrazine induces complete feminization and chemical castration in male African clawed frogs (Xenopus laevis). *Proceedings of the National Academy of Sciences of the United States of America* **107,** 4612–7 (2010).

19. Victor-Costa, A. B., Bandeira, S. M. C., Oliveira, A. G., Mahecha, G. A. B. & Oliveira, C. A. Changes in testicular morphology and steroidogenesis in adult rats exposed to Atrazine. *Reproductive Toxicology* **29,** 323–31 (2010).

20. Rooney, A. A. Matulka, R. a & Luebke, R. W. Developmental atrazine exposure suppresses immune function in male, but not female Sprague-Dawley rats. *Toxicological Sciences* **76,** 366–75 (2003).

21. Morgan, M. K., Scheuerman, P. R., Bishop, C. S. & Pyles, R. A. Teratogenic potential of atrazine and 2,4-D using FETAX. *Journal of Toxicology and Environmental Health* **48,** 151–68 (1996).

22. Shaw, G. New evidence for association of pesticides with Parkinson disease. *Neurology Today* **11,** 16–21 (2011).

23. Coban, A. & Filipov, N. M. Dopaminergic toxicity associated with oral exposure to the herbicide atrazine in juvenile male C57BL/6 mice. *Journal of Neurochemistry* **100,** 1177–87 (2007).

24. Hossain, M. M. & Filipov, N. M. Alteration of dopamine uptake into rat striatal vesicles and synaptosomes caused by an in vitro exposure to atrazine and some of its metabolites. *Toxicology* **248,** 52–8 (2008).

25. Filipov, N. M., Stewart, M. a, Carr, R. L. & Sistrunk, S. C. Dopaminergic toxicity of the herbicide atrazine in rat striatal slices. *Toxicology* **232,** 68–78 (2007).

26. Berman, S. B. & Hastings, T. G. Dopamine oxidation alters mitochondrial respiration and induces permeability transition in brain mitochondria: implications for Parkinson's disease. *Journal of Neurochemistry* **73,** 1127–37 (1999).

27. Miller, G. W., Gainetdinov, R. R., Levey, a I. & Caron, M. G. Dopamine transporters and neuronal injury. *Trends in Pharmacological Sciences* **20,** 424–9 (1999).

28. Howard, B. K. & Rohrich, R. J. Understanding the nasal airway: principles and practice. *Plastic and Reconstructive Surgery* **109,** 1128–46 (2002).

29. Yie W. Chien, Kenneth S. E. Su, Shyi-Feu Chang. Anatomy and physiology of the nose. In *Nasal Systemic Drug Delivery*, **1**; James Swarbrick; CRS Press: New York, 1989.

30. Dahl, R. & Mygind, N. Anatomy, physiology and function of the nasal cavities in health and disease. *Advanced Drug Delivery Reviews* **29,** 3–12 (1998).

31. Jones, N. The nose and paranasal sinuses physiology and anatomy. *Advanced Drug Delivery Reviews* **51,** 5–19 (2001).

32. Lane, A. P. Nasal anatomy and physiology. *Facial Plastic Surgery Clinics of North America* **12,** 387–95, v (2004).

33. Van Cauwenberge, P., Sys, L., De Belder, T. & Watelet, J.-B. Anatomy and physiology of the nose and the paranasal sinuses. *Immunology and Allergy Clinics of North America* **24,** 1–17 (2004).

34. Gerolymatos International S.A. Sinomarin -A nasal spray for nasal decongestion - a Gerolymatos International Product. at <http://www.sinomarin.com/nose_1.htm>

35. Illum, L., Farraj, N. F. & Davis, S. S. Chitosan as a novel nasal delivery system for peptide drugs. *Pharmaceutical Research* **11,** 1186–9 (1994).

36. Graff, C. L. & Pollack, G. M. Nasal drug administration: potential for targeted central nervous system delivery. *Journal of Pharmaceutical Sciences* **94,** 1187–95 (2005).

37. Illum, L. Is nose-to-brain transport of drugs in man a reality? *The Journal of Pharmacy and Pharmacology* **56,** 3–17 (2004).

38. Illum, L. Transport of drugs from the nasal cavity to the central nervous system. *European Journal of Pharmaceutical Sciences* **11,** 1–18 (2000).

39. Thorne, R. G. & Frey, W. H. Delivery of neurotrophic factors to the central nervous system: pharmacokinetic considerations. *Clinical Pharmacokinetics* **40,** 907–46 (2001).

40. Thorne, R. G., Pronk, G. J., Padmanabhan, V. & Frey, W. H. Delivery of insulin-like growth factor-I to the rat brain and spinal cord along olfactory and trigeminal pathways following intranasal administration. *Neuroscience* **127,** 481–96 (2004).

41. Zhang, H. Identification of membrane transporters to facilitate intranasal drug delivery using tissue-based and pharmacokinetic approaches. (PhD thesis, The University of Iowa, 2009).

42. Chemuturi, N. V. The characterization of bio-molecular processes Controlling dopamine transport across the nasal mucosa. (PhD thesis, The University of Iowa, 2005).

43. George, M. The role of organic cation transporters in the nasal uptake and brain distribution of organic cations substrates. (PhD thesis, The University of Iowa, 2013).

44. Schmidt, M. C., Dimen, D., Hilbe, M., Boderke, P., Ditzinger, G., Sandow, J., lang, S., Rubas, W. & Merkle, H. P. Validation of excised bovine nasal mucosa as in vitro model to study drug transport and metabolic pathways in nasal epithelium. *Journal of Pharmaceutical Sciences* **89,** 396–407 (2000).

45. Himanshu, R., Jakir, P., Pradnya, H., Suneel, P. & Rahul, S. The impact of permeability enhancers on assessment for monolayer of colon adenocarcinoma cell Line (Caco-2) Used in Vitro. *Journal of Drug Delivery & Therapeutics* **3,** 20–29 (2013).

46. Kandimalla, K. K. Carrier mediated transport of small molecules across bovine nasal mucosae: implications in nose-to-brain drug delivery. (PhD thesis, The University of Iowa, 2004).

47. Vasiliou, V., Vasiliou, K. & Nebert, D. W. Human ATP-binding cassette (ABC) transporter family. *Human Genomics* **3,** 281–90 (2009).

48. Herkenne, C., Naik, A., Kalia, Y. N., Hadgraft, J. & Guy, R. H. Effect of propylene glycol on ibuprofen absorption into human skin in vivo. *Journal of Pharmaceutical Sciences* **97,** 185–97 (2008).

49. Liao, S. L. Part I. Use of a laser/photodiode array system to study transport of 4-nitrophenol across silicone rubber membranes. Part II. A generic microcomputer-based electroanalytical system. (PhD thesis, The Ohio State Univesity, 1991).

50. Roghair, Pei-Fen, C. The role of solution tonicity and water flux on intranasal absorption. (PhD thesis, The University of Iowa, 2001).

51. Shimoda, N., Maitani, Y., Machida, Y. & Nagai, T. Effects of dose, pH and osmolarity on intranasal absorption of recombinant human erythropoietin in rats. *Biological & Pharmaceutical Bulletin* **18,** 734–9 (1995).

52. Suber, R. L., Deskin, R., Nikiforov, I., Fouillet, X. & Coggins, C. R. Subchronic nose-only inhalation study of propylene glycol in Sprague-Dawley rats. *Food and Chemical Toxicology* **27,** 573–83 (1989).